University of Nebraska - Lincoln
DigitalCommons@University of Nebraska - Lincoln

Dissertations & Theses in Earth and Atmospheric Sciences

Earth and Atmospheric Sciences, Department of

Summer 8-15-2015

EVALUATION OF REGIONAL CLIMATE MODELS WITH REMOTELY SENSED EVAPOTRANSPIRATION DATA

Doruk Ozturk
University Of Nebraska-Lincoln, doruk@huskers.unl.edu

Follow this and additional works at: http://digitalcommons.unl.edu/geoscidiss

 Part of the Hydrology Commons, Natural Resources and Conservation Commons, and the Water Resource Management Commons

Ozturk, Doruk, "EVALUATION OF REGIONAL CLIMATE MODELS WITH REMOTELY SENSED EVAPOTRANSPIRATION DATA" (2015). *Dissertations & Theses in Earth and Atmospheric Sciences*. 67.
http://digitalcommons.unl.edu/geoscidiss/67

This Article is brought to you for free and open access by the Earth and Atmospheric Sciences, Department of at DigitalCommons@University of Nebraska - Lincoln. It has been accepted for inclusion in Dissertations & Theses in Earth and Atmospheric Sciences by an authorized administrator of DigitalCommons@University of Nebraska - Lincoln.

EVALUATION OF REGIONAL CLIMATE MODELS WITH REMOTELY SENSED EVAPOTRANSPIRATION DATA

by

Doruk Ozturk

A THESIS

Presented to the Faculty of

The Graduate College at the University of Nebraska

In Partial Fulfillment Requirements

For the Degree of Master of Science

Major: Earth and Atmospheric Sciences

Under the Supervision of Professors Robert Oglesby and Ayse Kilic

Lincoln, Nebraska

August, 2015

EVALUATION OF REGIONAL CLIMATE MODELS WITH REMOTELY SENSED EVAPOTRANSPIRATION DATA

Doruk Ozturk, M.S.

University of Nebraska, 2015

Advisers: Robert Oglesby and Ayse Kilic

Water is one of the most precious resources on Earth. Managing water resources is a complex discipline that requires accurate data, which in turn means that the management of water resources is limited by the availability and quality of these datasets. Evapotranspiration (ET) is one of these key datasets, but is also one that is lacking in large-scale spatial distribution with traditional methods such as weighing lysimeters or Bowen ratio. This is a quantity that needs to be evaluated in regional and global climate models since it is a substantial component of the land surface-atmosphere interaction. In order to overcome the limitations imposed by point wise calculation of ET, a new dataset based on a surface energy balance model Mapping Evapotranspiration at High Resolution with Internalized Calibration (METRIC) constrained by Moderate Resolution Imaging Spectroradiometer (MODIS) satellite imagery have been developed. A Fully Automated Python implementation of METRIC model, as well as a script which generates 15-day Reference ET Fraction (ETrF) composites were needed and developed to cover the Contiguous United States (CONUS) due to the high computational time for manual processing of METRIC. In this study, the new ET dataset will be used to evaluate how well the Weather Research and Forecasting Model, coupled with Community Land Model's (WRF-CLM) as well as Noah-MP and Bucket Land Surface Model, evaluate ET.

CLM, Noah-MP and Bucket are the models used to understand the processes between land and atmosphere and also climate change, and contain crucial but poorly known parameterizations for ET.

Dedicated to my parents and Hazal Canisag

Acknowledgement

Upon completing this dissertation, I am indebted to many people who helped me and made this possible. First and foremost, I would like to thank my advisors, Robert Oglesby and Ayse Kilic for their guidance and encouragement in every stage of the completion of my thesis. Their passions for research, dedications to work and wise perspectives greatly inspired me. I would also like to express my appreciation to the other member of my committee, Vitaly Zlotnik for his suggestions and serving on my committee. Particularly, I would like to thank Cynthia Hays for her help with the WRF runs and Dr.Richard Allen for sharing his model and insights.

I am truly grateful to receive assistance and advice from our research group. A special thank to Hazal Canisag for being a support system throughout the entire time I spent in graduate school. She was always helpful and patient. She encouraged me when I was tired and she was always there as a listener. This thesis would not have been possible without her.

Most importantly, none of these would have been possible without the support of my family. I owe them much.

Last but not least, I would like to thank all my friends for being always there to cheer me on and to support me.

Table of Contents

List of Figures

List of Tables

CHAPTER 1: INTRODUCTION

Evapotranspiration (ET) is a major component of the hydrological cycle which affects climate processes and agricultural practices. Large amounts of water vapor are lost via ET, and this process redistributes heat and water into the atmosphere. The partitioning of ET to transpiration and evaporation is dependent on leaf area index (LAI). Vegetated areas with greater LAI have higher transpiration rates as opposed to evaporation from soil surfaces (Bethenod et al., 2000). This makes ET a major concern for the agricultural areas and climate models in general. In order to estimate ET, several frameworks exist, and the most widely-accepted ones employ surface energy balance methods. Satellite based models, such as Surface Energy Balance Algorithm (SEBAL) developed by Bastiaanssen et al. (1998) or Mapping Evapotranspiration at High Resolution using Internalized Calibration (METRIC) developed by Allen et al., 2007 a&b, provide spatially continuous datasets to estimate ET as a residual of the surface energy balance. Wind speed, solar radiation, humidity and air temperature at the surface, are used to calculate reference evapotranspiration (Walter et al., 2000), while satellite imagery is used to generate a crop coefficient-like coefficient with METRIC. The necessary weather parameters are obtained from the North America Land Data Assimilation System (NLDAS, Mitchell et al., 2004). METRIC estimates actual ET without quantifying complex hydrological processes and without identifying crop types, which eases the process. Crop type information is not sufficient since it is used only for surface roughness parameters, which is handled in METRIC with a function that is dependent on LAI.

However, all of these satellite-based techniques that use land surface temperature from satellites and do not use microwave, have a downside, which are the clouds. Cloud cover makes it challenging to obtain complete, seamless ET datasets. METRIC is intended to run with high-resolution satellite imagery (Landsat) at 30 meters due to the fact that selecting homogeneous anchor pixels are suitable with that resolution for calibrating the model. For relatively large domains, however, usage of MODIS is more suitable since the areal coverage is greater than Landsat. For this study due to the size of the domain, MODIS was selected rather than Landsat.

Approximately 70 per cent of the incoming radiation over land is absorbed by the surface (Myneni et al., 1992). Regional Climate Models (RCMs) provide sophisticated land surface physics schemes which models surface processes as well as ET, coupled with climate models such as Weather Research and Forecast (WRF) model (Michalakes et al., 2004; Cai et al., 2014, McCoy et al., 2009). RCMs provide means to understand the interactions between the atmosphere, land surface and vegetation. Better estimates of ET should improve both real-time and forecasted climate predictions, which in turn should yield to better climate change research and better water resources management practices.

The Community Land Model (CLM), developed by Oleson et al., 2010 serves as the state-of-art land surface parameterization tool for climate models. On the other hand, Multi-Physics version of the Noah (Noah-MP) developed by Nie et al., 2011 is an alternative to CLM. A multi-layer soil temperature model for mm5 (Bucket) developed by Dudhia et al., 1996 with both grass and default vegetation options are conducted to pinpoint the differences between land surface physics models.

Precipitation is another major component of the hydrological cycle. It occurs as a function of the available moisture in the atmosphere, which is closely related with ET on regional scale. In order to represent the hydrological cycle realistically those two parameters should be estimated carefully. Parameter elevation Regression on Independent Slopes Model (PRISM) developed by Daly et al., 1997 is used in this study to validate the precipitation products, which is assumed to be the ground truth.

CHAPTER 2: OBJECTIVES

The aim of this study is to evaluate and compare ET values generated by different land surface schemes with METRIC model. Improved evaluation of ET could substantially improve the climate simulations. For instance, better predictions could help the determination of the planting, harvesting or irrigation time, which will stimulate the economy by increasing the yield and productivity by consuming the least amount of natural resources possible. Part of the objective is also to compare the precipitation products to see how well the models do, since precipitation is highly related with ET. Specific objectives of this study are to:

- Evaluate ET products that are generated with METRIC and land surface schemes coupled with WRF
- Conduct statistical analysis to estimate significance of the differences between models
- Investigate sensitivity of ET to differences in land use classes
- Develop a better calibration scheme in METRIC to produce large area ET products from MODIS

CHAPTER 3: METHODS

Three years are selected to conduct this study; 2005 (a normal year), 2007 (a wet year) and 2012 (a dry year). For 2005 CLM ET results are compared with METRIC ET results. For 2007 and 2012, Noah-MP and Bucket ET values are compared with METRIC ET. Four months (May, June, July, August), when ET peaks, are selected for the comparison. Only monthly values were compared due to the massive amounts of data generated. Figure 1 shows the domain that is used in this study. This is a large enough domain that will provide sufficient comparison information between models.

The spatial analysis shows WRF-CLM is underestimating ET compared to METRIC overall. For the sake of accuracy, contaminated pixels that are detected by cloud mask are not used in this study. For every month period there were two METRIC ETrF products, which is assumed to be constant throughout the fifteen day period. To get the monthly values those ETrF values were multiplied by reference ET values for every day, which resulted in fifteen actual ET maps. During the accumulation procedure to get monthly values from daily values, there are some pixels which are contaminated for the first fifteen-day period of a month, but cloud-free for the second fifteen day period of a month. In that case those pixels were dropped from the calculations to increase the confidence levels with METRIC. In other words, only the pixels that are cloud free for both ETrF maps for a month are used. Even if some pixels were dropped, at least fifty thousand comparison pixels were present for every month for every year, which is sufficient to conduct a comparison study.

3.1. Domain Description

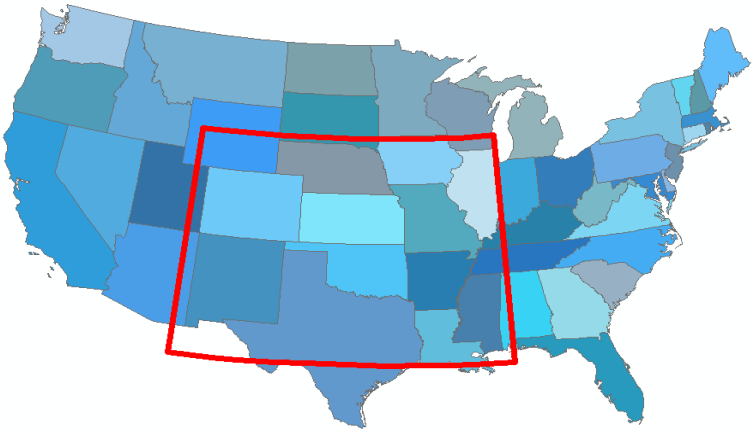

Figure 1. Domain that is used to conduct ET comparisons

Figure 1 shows the domain that is used for this study. It covers the High Plains Region with a 4km pixel resolution for WRF which is outlined with red color in Figure 1.

3.2. Input Dataset Description

3.2.1. Moderate Resolution Imaging Spectroradiometer (MODIS)

The MODIS instrument platform on the Terra satellite is used during this study to generate ET products. MODIS-Terra has the advantage of high temporal resolution compared to Landsat, which makes it possible to work on the daily scale for large domains such as entire contiguous United States (CONUS). This kind of work is not possible with satellites such as Landsat that have less frequent revisits. Four MODIS products are used in this study. The calibrated radiance product at 1 km resolution (MOD021KM) is used to calculate surface reflectance as well as albedo and some

vegetation indices such as normalized difference vegetation index (NDVI, Tucker et al., 1979) and Normalized Difference Water Index (NDWI, Gao et al., 1996). The geolocation field product at 1 km resolution (MOD03) is used to calculate the solar zenith and sensor zenith angles. The land surface temperature and emissivity product at 1 km resolution (MOD11_L2) is used to calculate the land surface temperatures as well as getting the view angle of the sensor. The cloud mask product at 1km (MOD35_L2) is used to identify the cloudy pixels to mask them out. Details and algorithms of MODIS implementation into METRIC model can be found in Trezza et al., 2013. All MODIS datasets are reprojected to Albers Equal Area Conic Projection using Geospatial Data Abstraction Library (GDAL) with 1 km resolution. All the MODIS data has been downloaded using NASA's ftp servers.

In order to have a full coverage of the domain MODIS platform's Terra satellite is used due to the high temporal resolution. The procedure introduced in Trezza et al., 2013 were followed to operate METRIC with MODIS.

3.2.2. NLDAS

NLDAS is used as a complementary dataset during the calculation of reference ET. Reference ET requires air temperature, humidity, solar radiation and wind speed. All of these datasets are found in NLDAS in hourly fashion for the entire CONUS. American Society of Civil Engineers' standardized reference evapotranspiration equation for alfalfa is used in this study since alfalfa reference ET (Walter et al., 2000) values reflect the

conditions of agricultural crops better. NLDAS is reprojected to Albers Equal Area Conic Projection using GDAL with 12km resolution. NLDAS forcing 2 model is used in this study also for the precipitation comparisons with PRISM datasets to check the accuracy of precipitation datasets even though orographic adjustment of the dataset was done with PRISM. The North American Regional Reanalyzes (NARR) dataset was used to generate NLDAS dataset. Surface downward shortwave radiation is bias corrected and this eliminated the need for a quality assurance and control analysis for calculation of reference evapotranspiration. Downward shortwave radiation needs to be corrected in case of systematic errors, which means a sensor failure rather than cloudy conditions. This bias should be corrected since it does not represent cloudy conditions.

3.2.3. Digital Elevation Model, Land Use and Soil Data

The Shuttle Radar Topography Mission (SRTM) Digital Elevation Model (DEM) is used to provide elevation information in METRIC. This dataset was aggregated to 1 km pixel size to match and align MODIS-Terra.

The National Land Cover Database (NLCD-2006, Homer et al., 2012) is used as the land use product for this study. This dataset was to 1 km pixel size to match and align MODIS-Terra. This dataset has 18 different classes that cover the CONUS domain. This dataset is also used to compare error statistics from different land use types between WRF and METRIC products since it has approximately 80 percent accuracy (Wickham et al. (2013)). Figure 2 and Figure 3 shows the land use maps that are used in METRIC and WRF models.

The Statsgo2 database (Schwarz et al., 1995) is used to obtain the necessary soil parameters such as wilting point, available water capacity and field capacity. Those parameters are used to estimate the evaporation from bare soil (Allen et al., 2005).

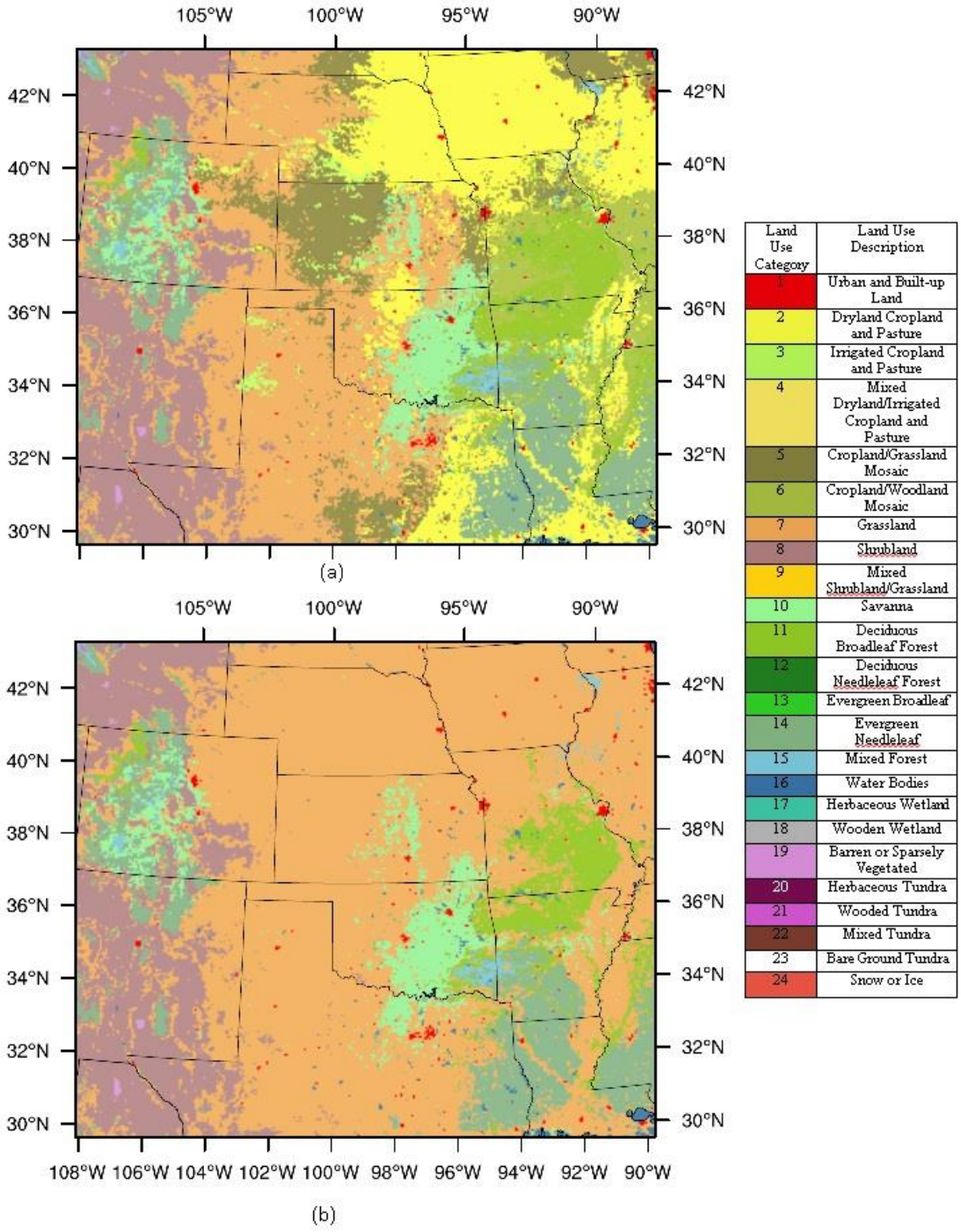

Figure 2. Land use map for (a) Noah-MP, CLM and Bucket Default Vegetation models (b) Bucket Grass Vegetation Model

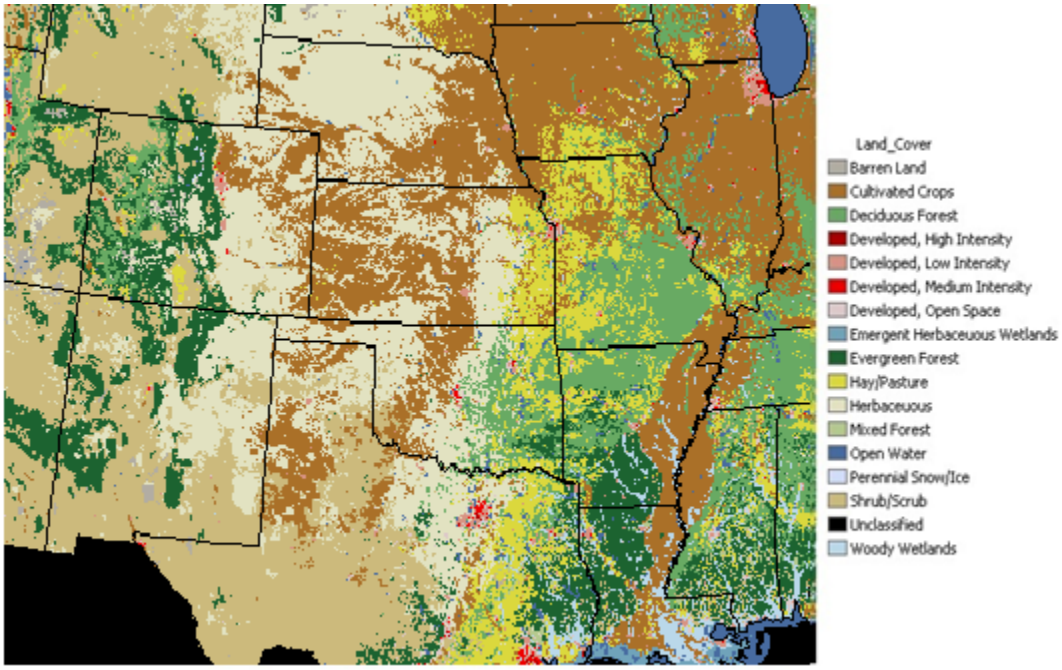

Figure 3. Land use map that is used with METRIC (NLCD-2006)

3.2.4. NARR

Large-scale lateral forcing and initial conditions are obtained from the North American Regional Reanalyses (NARR), which is developed by Mesinger et al., 2006, at 32 km spatial resolution for WRF simulations. NARR has 3-dimensional atmospheric data, surface data and fixed-field data. NARR's data coverage is from 1979 to near present in 3 hourly format. It has 29 pressure levels. Reanalysis datasets such as NARR is very useful to create initial conditions for regional climate models (Bukovsky et al., 2007).

3.2.5. PRISM

PRISM dataset uses the elevation as the dependent variable for the calculations. Daly et al., 1994 applied a statistical approach to interpolate station observations and generate a distributed dataset. PRISM data is downloaded from PRISM Climate Group, Oregon State University (http://prism.oregonstate.edu). Prism has 4 km spatial resolution.

For precipitation comparisons, the PRISM dataset is assumed to represent ground truth. PRISM was selected because it is one of the most accurate precipitation products for CONUS (Grant et al., 2013, DiLuzio et al., 2007). As stated before precipitation and evapotranspiration are highly related. Even if the focus of this study is

evapotranspiration, comparison of precipitation products may provide helpful insight about WRF-METRIC differences in ET.

3.3. Model Description

3.3.1. METRIC

METRIC is a simulation tool that can be used to estimate ET with incorporation of satellite technology. There are four major components of the surface energy balance. LE is the latent heat flux (W/m2), Rn is the net radiation flux (W/m2), G is the soil heat flux (W/m2) and H is the sensible heat flux (W/m2).

$$LE = R_n - G - H \qquad (1)$$

The net radiation flux represents the total available energy for land, atmosphere and water bodies. Soil heat flux is energy passing through the soil due to conduction. There is an inverse relationship between soil heat flux and leaf area index since canopy cover decreases the albedo.

$$R_n = R_{s\downarrow} - \alpha R_{s\downarrow} + R_{L\downarrow} - R_{L\uparrow} - (1 - \varepsilon_0) R_{L\downarrow} \qquad (2)$$

Where $R_{s\downarrow}$ is incoming short-wave radiation (W m^{-2}), α is albedo (dimensionless), $R_{L\downarrow}$ is incoming long-wave radiation (W m^{-2}), $R_{L\uparrow}$ is outgoing long-wave radiation (W m^{-2}) and ε_0 is the broad-band surface thermal emissivity.

The absorption of sunlight by the air causes a heat temperature difference. There is no phase change during this process and it is called sensible heat flux. Latent heat flux is the rate of latent heat loss due to the evapotranspiration and a phase change happens during this process.

With METRIC an instantaneous reference ET fraction (ETrF) product is obtained for the satellite pass time. Reference ET is calculated in hourly steps with NLDAS. A constant ETrF was assumed for a fifteen-day period which means, reference ET controlled the daily changes in the actual ET. For every fifteen days one ETrF composite was generated using satellite images. Then using NLDAS, reference ET was calculated with daily time steps. Finally the generated ETrF composite was multiplied with 15 different reference ET datasets for each day, which yields actual ET data in daily time steps. While preparing the ETrF maps for the fifteen day periods, cloudy pixels were discarded. Mean ETrF values were then calculated for the overlapping ETrF pixels by also discarding the pixels which has a greater view angle than 30 degrees. This approach secured the quality of the ETrF values since high view angles alter the pixel quality. An instant of this case is shown in Figure 4. One can see the missing points in the southern part of the map which are the results of clouds. Some of the pixels are calculated with up to four different ETrF values and some are only one value.

During the calculation of sensible heat flux a novel methodology was developed to divide the MODIS images into 150x150 km parcels. For every parcel, a vertical temperature gradient was calculated independently. This approach was applied due to the large areal coverage of MODIS images. Usage of a single temperature gradient would not

be representative for the entire image. For every parcel two anchor pixels are selected. One is a hot pixel and the other is a cold pixel. Temperature gradient is assumed to be known within those 2 extreme pixels, which makes it possible to do an inverse solution to calculate a map of temperature gradient. It is a linear regression operation. If the MODIS images are not divided into blocks, the hot anchor pixel will always be coming from south and the cold pixel will be coming from north since selecting criteria for those extreme pixels are temperature and NDVI. Using only 2 anchor pixels for an entire MODIS imagery is not a realistic scenario, since the temperature gradient will be dependent upon longitude. A python-based routine of METRIC is implemented to overcome this issue since manual implementation of this methodology is extremely time consuming. The 150 km parcel size is selected since Landsat images size approximately 150x150 km and METRIC was successfully ran with Landsat images using single temperature difference coefficients. H is calculated with the following formula for every block individually.

$$H = \rho_{air} C_p \frac{dT}{r_{ah}} \qquad (3)$$

Where ρ_{air} is air density (kg m^{-3}), C_p is specific heat of air at constant pressure (J kg^{-1} K^{-1}), r_{ah} is aerodynamic resistance (s m^{-1}) between two near surface heights (0.1 and 2 meters) and *dT* is the near surface temperature difference between that two height which is mentioned. *dT* is calculated using the two anchor pixels and as mentioned an inverse solution is conducted to generate a *dT* map for the entire block.

$$\frac{G}{R_n} = 0.05 + 0.18e^{-0.521\,LAI} \quad (LAI \geq 0.5) \qquad (4)$$

$$\frac{G}{R_n} = 1.80\frac{(Ts-273.15)}{R_n} + 0.084 \quad (LAI < 0.5) \qquad (5)$$

Using this empirical equations soil heat flux is calculated. In order to calculate soil heat flux, net radiation has to be calculated first. Then based on the LAI values, soil heat flux can be calculated.

As with all models METRIC has its own limitations. Perfect accuracy should not be expected. Especially with the MODIS pixel size it can be challenging to find the anchor pixels for the *dT* calculation.

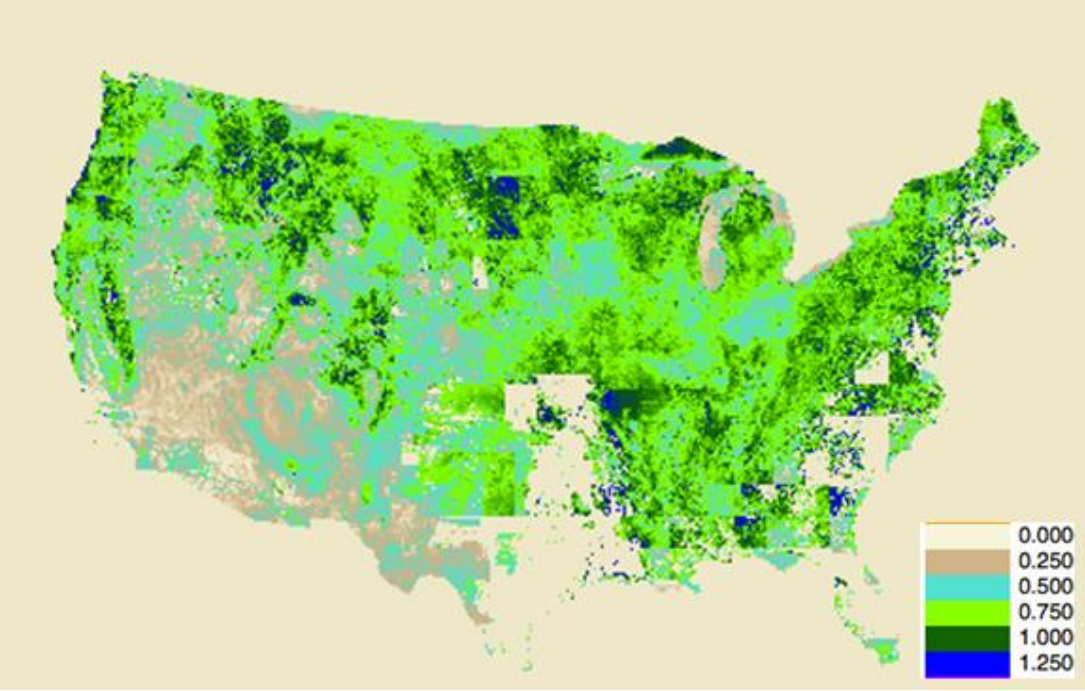

Figure 4. ETrF product for the period between 1st of June and 15th of June, 2007

3.3.2. CLM

CLM is a land surface model that handles the interactions between atmosphere and land. It is a community developed model and it can be coupled with atmospheric models such as WRF. Conservation of energy, water and carbon is considered in the model. That means both hydrological and surface energy budgets and balance methods are conducted inside the model. The processes simulated include: absorption, reflection and transmittance of solar radiation, surface energy balance components, and heat transfer in soil, soil hydrology and dynamic land cover change. The model calculates surface energy, momentum and radiative fluxes using soil hydrologic states from the previous time step. Then the land model updates soil hydrology calculations based on these fluxes. Even if there is enough energy to generate evapotranspiration, if there is no soil moisture present in the soil, there is no ET. A linear model is developed to estimate smaller time step for leaf area index products between monthly MODIS leaf area index images. The model calculates transpiration and evaporation independently. Sensible and latent heat fluxes are calculated differently for vegetated and non-vegetated surfaces. Vegetation state of a pixel is defined by the leaf area index and stem index. Sensible heat flux is dependent on vegetation, surface temperature, and specific humidity.

3.3.3. Noah-MP

Noah-MP runs are conducted without the dynamic vegetation option. For vegetated and non-vegetated surfaces different algorithms are applied, and classification is done by using leaf area index and stem area index. Vegetation temperature and ground temperature are separated in this model. A short-term leaf dynamic model to simulate LAI and vegetation greenness fraction was added to Noah-MP. Other than those facts it uses Noah as a base model. Also there are multiple common features between CLM and Noah-MP. Details of the model are not the concern of this study and they can be found in the model documentation.

Noah-MP and CLM are considered to be the advanced land surface schemes in the land surface modeling literature according to Cai et al., 2014. There are two major differences between CLM and Noah-MP. The first one is how the vegetation is handled. In CLM there are up to 10 vegetation types in one grid cell and the LAI is prescribed. In Noah-MP, dominant vegetation type in one grid cell with dynamic LAI option is offered. The second difference is the soil layers. CLM has 10 layer moisture and 15 layer temperature profiles. Noah-MP has four layers both for the moisture and the temperature.

3.3.4. BUCKET

This model divides the top layer into two slabs. The components of the surface energy balance forces the top slab to change its temperature to vary. The Bucket model is run in two modes, with default vegetation option or grass option. The difference between this model and CLM or Noah-MP is the complication of how vegetation and vegetation related issues are handled. CLM and Noah-MP conduct much more realistic scenarios compared to the bucket model. Details of the model are not the concern of this study and they can be found in the model documentation. This model is called a bucket model because it is similar to a hydrological bucket. One can visualize this model as a bucket where there is input, output and storage of water. This model is estimating evaporation with good accuracy since it can be calculated with a bucket hydrology type of model, but fails with transpiration since it requires complex formulation of the surface energy balance.

CHAPTER 4: RESULTS AND DISCUSSION

In order to ease the process of comparison, land use map is used to find which land use types the two models agree/disagree. A majority function that assigns the most frequent value within a given resolution is used to bring 30 m NLCD product to 4 km land use map. The threshold in this function is 51 % by default, which means within that 4 km pixel, if more than half of the values belong to one land use class, that land use class is assigned to the 4 km pixels. With METRIC, the most confidence is present for land uses through 41 to 95 (see Table 1), which are agricultural and naturally vegetated land use classes as well as wet lands. The reason for that is the reference ET calculation which is for alfalfa. For the analysis, therefore, the focus will be on the vegetated areas.

4.1. Spatial Comparisons

4.1.1. Comparison for 2005

For 2005, in general WRF-CLM underestimates the ET values. As expected, both models produced the highest ET result during June and July. For the precipitation products, NLDAS agrees well with PRISM dataset, not surprising since NLDAS precipitation product was calibrated with PRISM dataset. WRF-CLM precipitation has some different spatial patterns compared to PRISM but the magnitudes of precipitation

agree fairly well. WRF-CLM ET spatially follows the precipitation product, since the only input for its hydrology module is precipitation. According to the WRF-CLM model, if there is not sufficient precipitation, there is not enough soil moisture to generate ET. That is the primary reason that WRF-CLM ET product has the same spatial patterns as the precipitation product. That is not the case with METRIC. With METRIC the satellite acquires the imagery and the ET product is calculated for that very moment. Precipitation affects the soil moisture in METRIC for the hot anchor pixel. The instantaneous image is only partially affected by the precipitation because if there is a precipitation event, this means that portion of the image is cloudy and there is no data to retrieve. Figure 5-12 shows ET and precipitation products for 2005 May, June, July and August.

For the 4 months considered, monthly values are calculated to compare the total amount of ET for a month. The same kind of aggregation was also done for precipitation data. METRIC is generating greater ET values compared to WRF-CLM. Both models generated the highest ET on June and July, which is to be expected due to the peak in incoming net radiation. Spatial patterns between WRF and METRIC ET were not similar. Magnitudes are also different. Spatial comparisons showed there is no trend or correlation between METRIC and WRF-CLM. Figure 5 compares the difference between WRF-CLM ET and METRIC ET. One statement that can be made is the homogeneity in the WRF-CLM map which does not look realistic for Nebraska. With METRIC forest and agricultural land use classes have higher ET values.

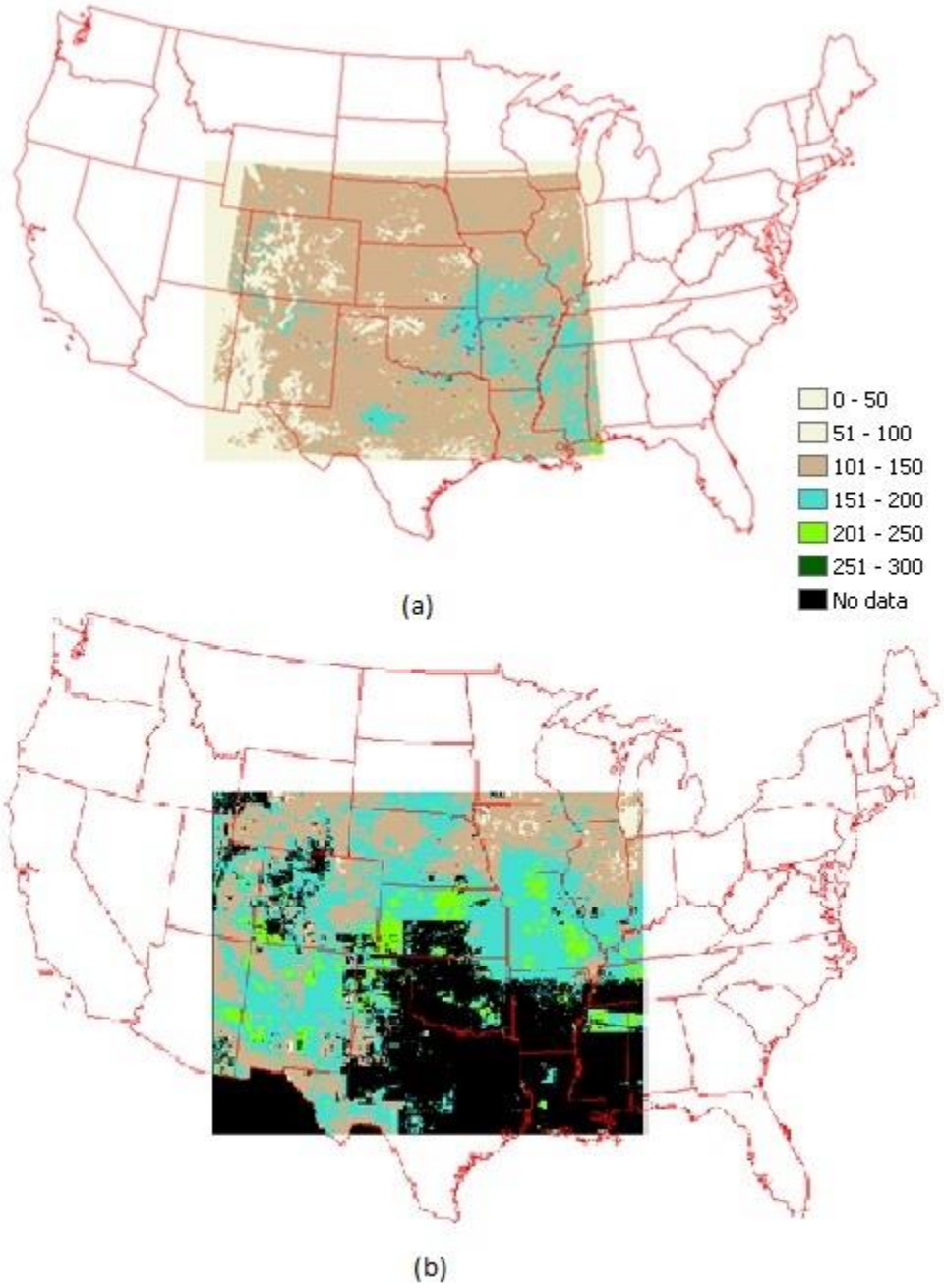

Figure 5. Monthly ET values for (a) WRF-CLM and (b) METRIC for May, 2005 (mm)

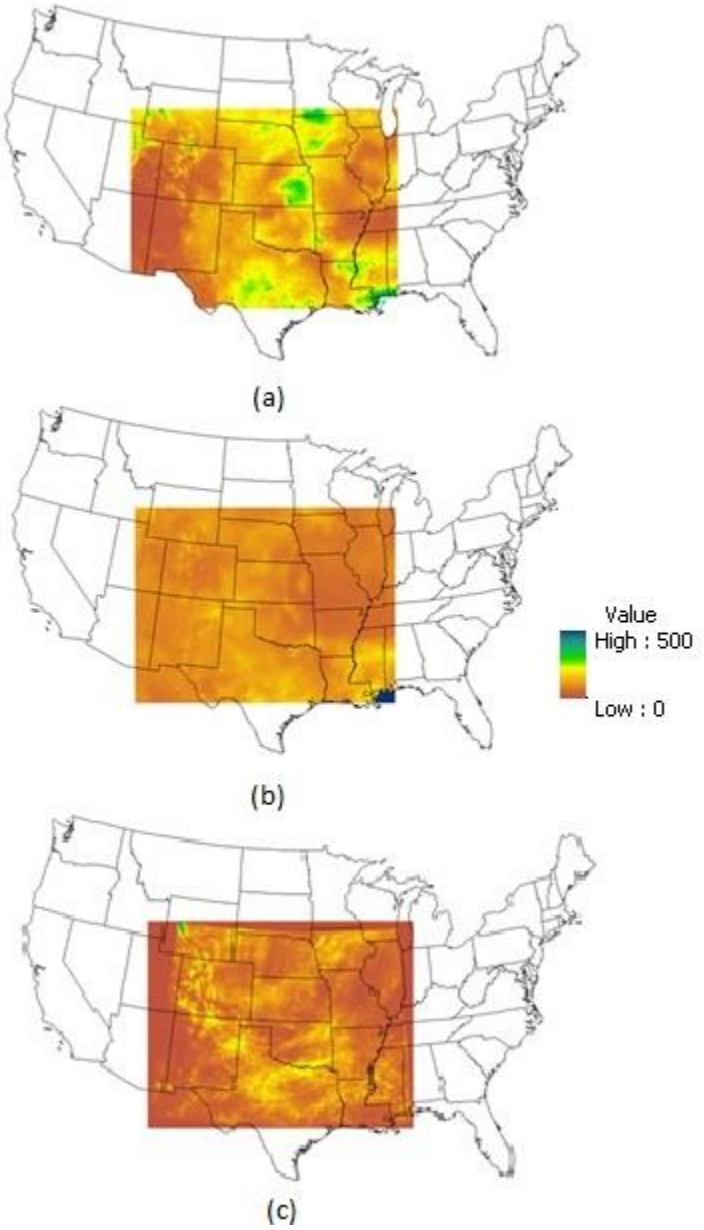

Figure 6. Monthly precipitation values for (a) PRISM, (b) METRIC-NLDAS and (c) WRF-CLM for May, 2005 (mm)

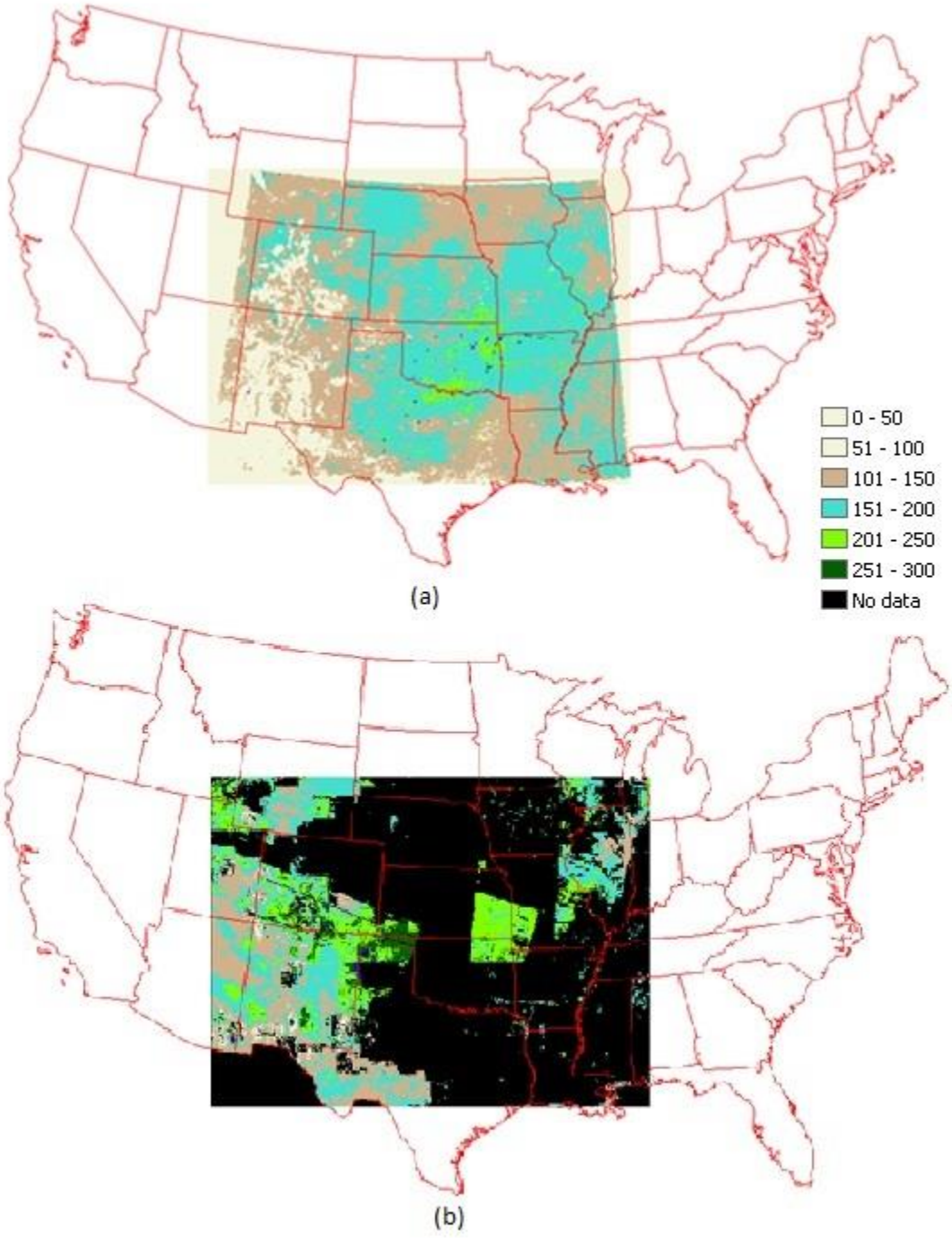

Figure 7. Monthly ET values for (a) WRF-CLM and (b) METRIC for June, 2005 (mm)

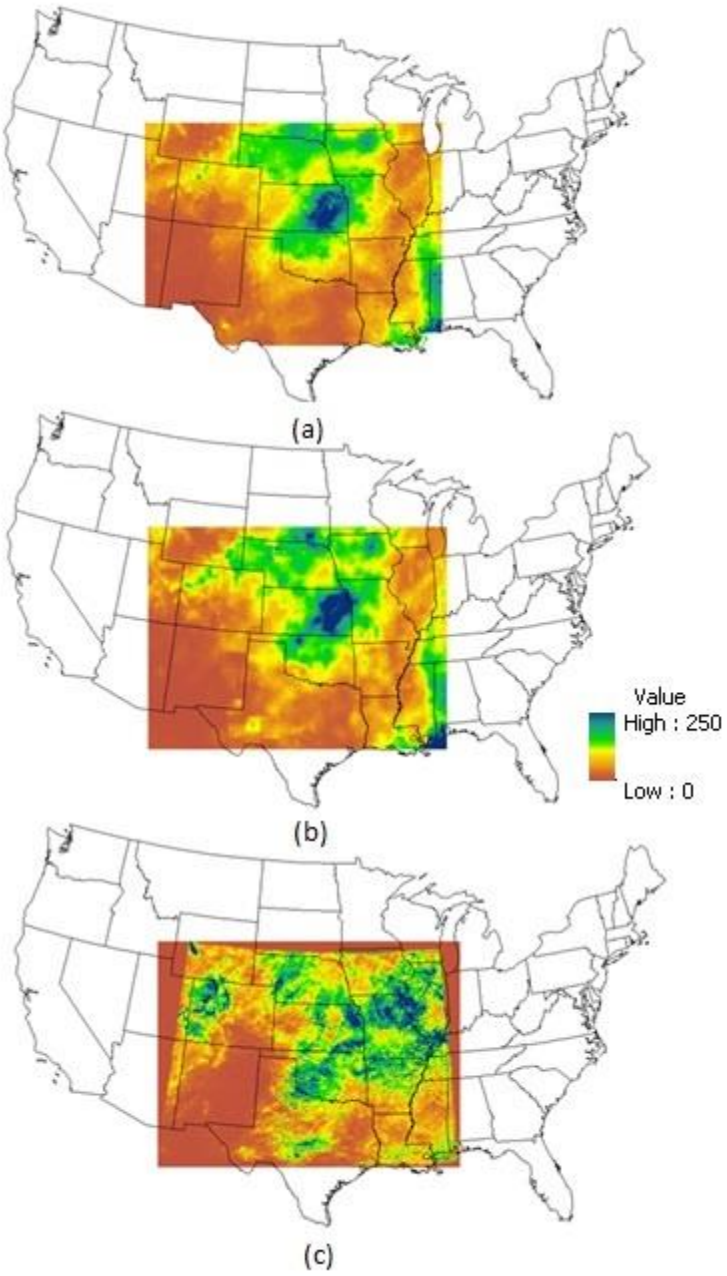

Figure 8. Monthly precipitation values for (a) PRISM, (b) METRIC-NLDAS and (c) WRF-CLM for June, 2005 (mm)

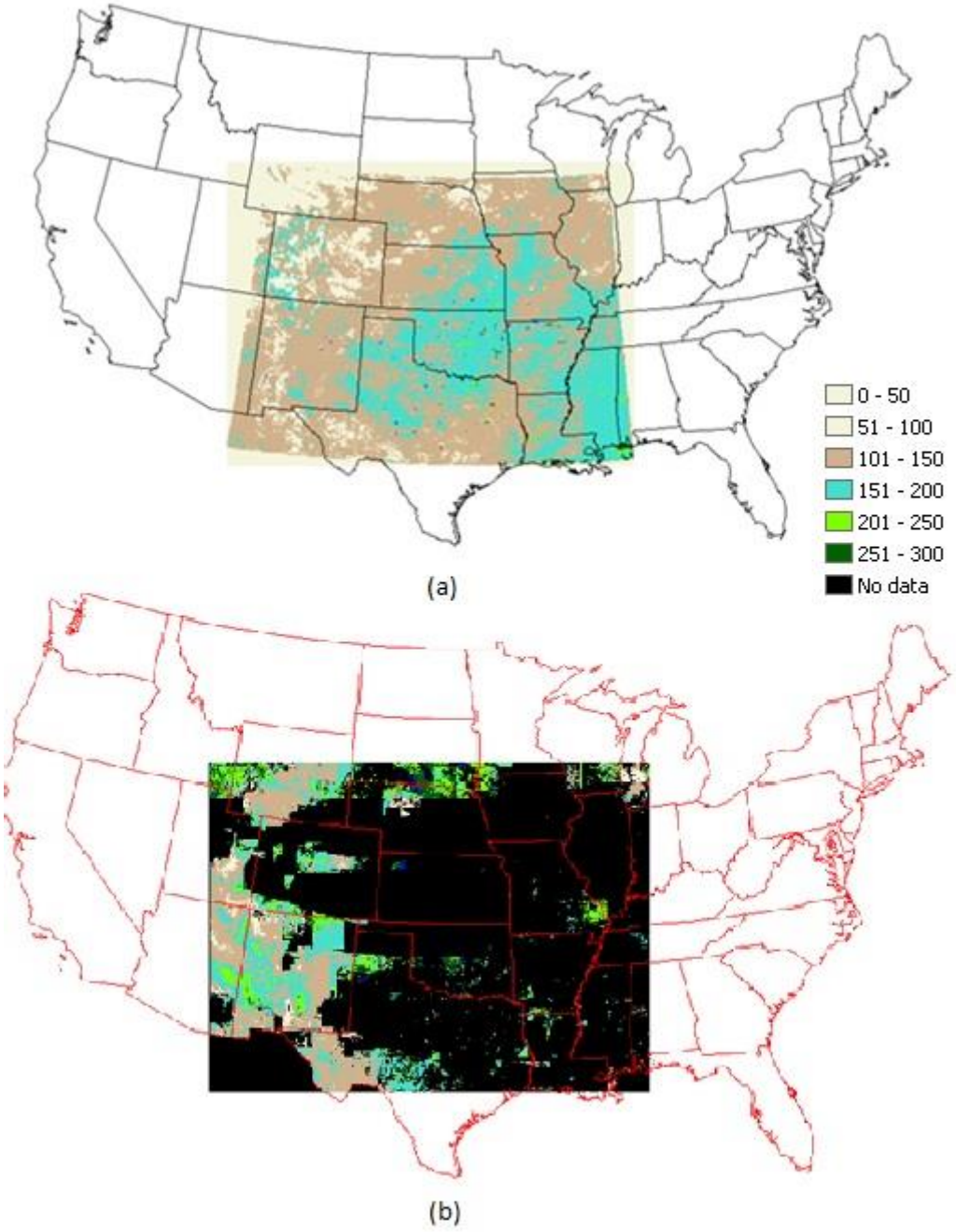

Figure 9. Monthly ET values for (a) WRF-CLM and (b) METRIC for July, 2005 (mm)

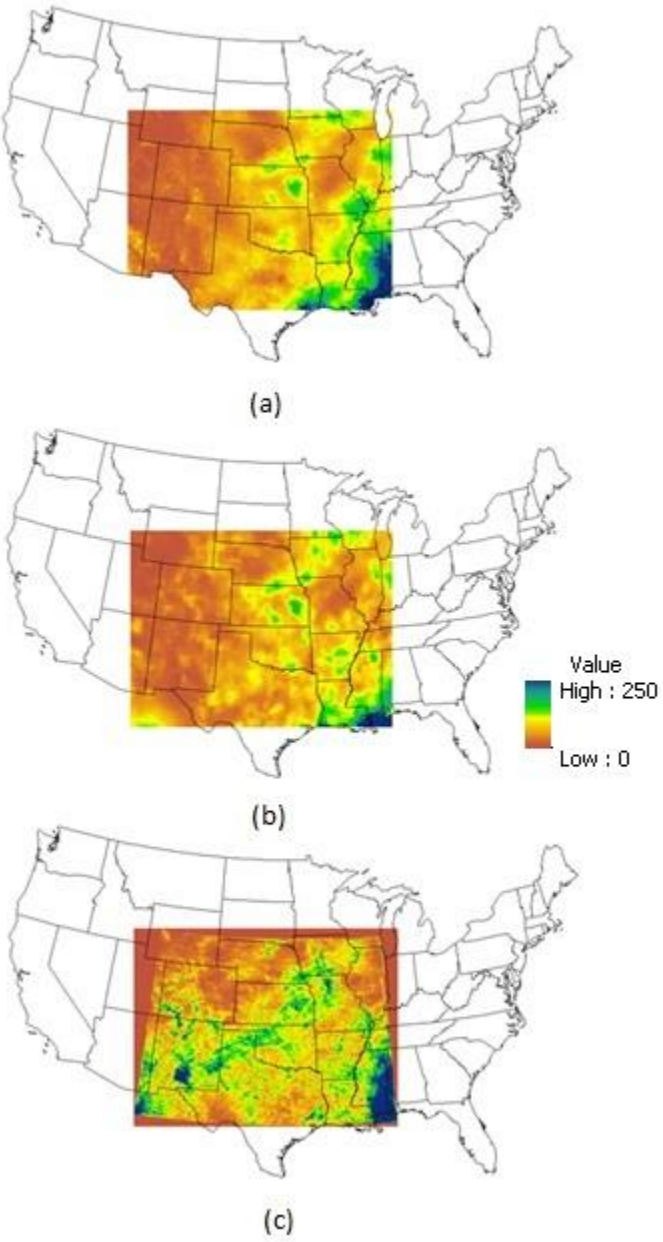

Figure 10. Monthly precipitation values for (a) PRISM, (b) METRIC-NLDAS and (c) WRF-CLM for July, 2005 (mm)

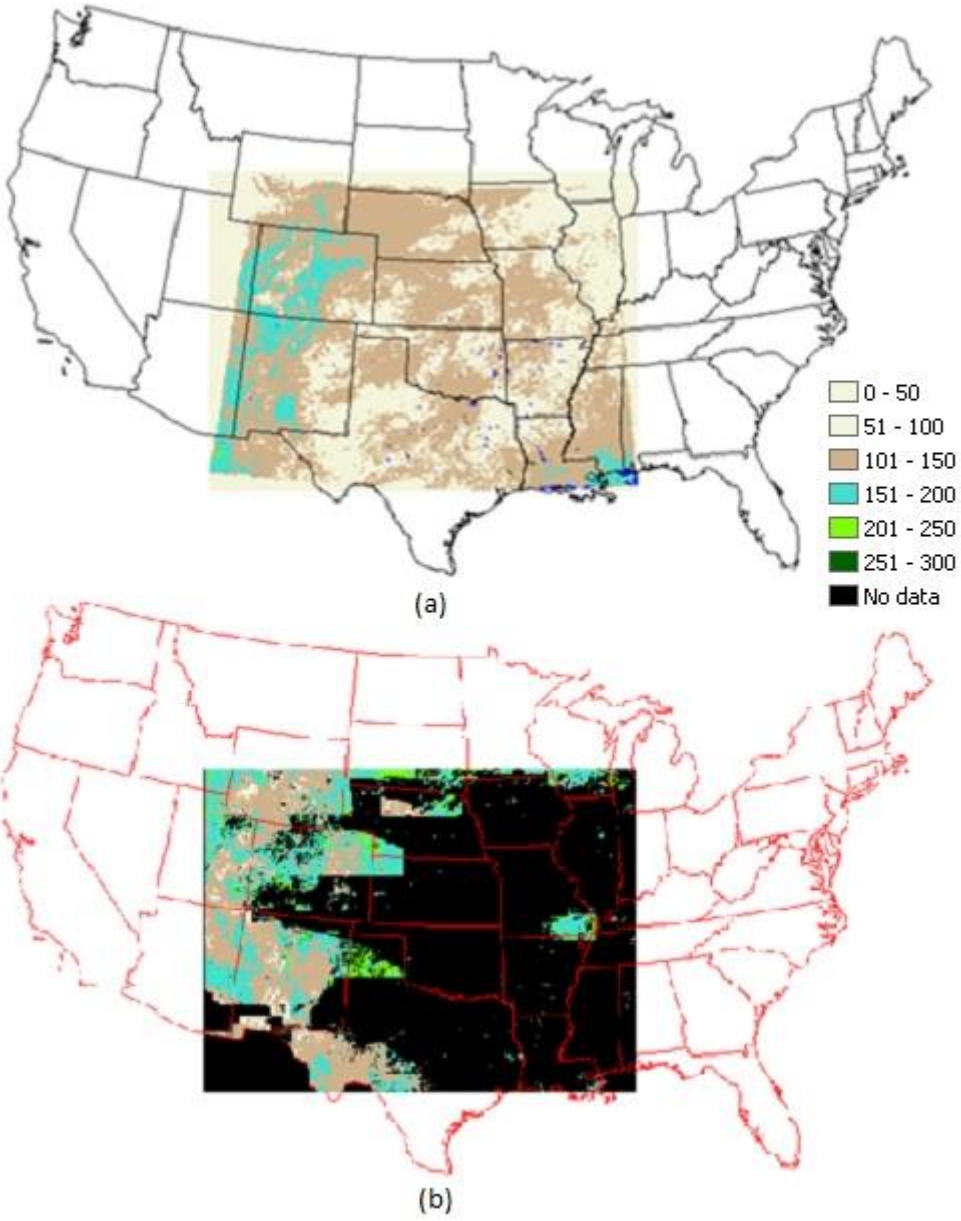

Figure 11. Monthly ET values for (a) WRF-CLM and (b) METRIC for August, 2005 (mm)

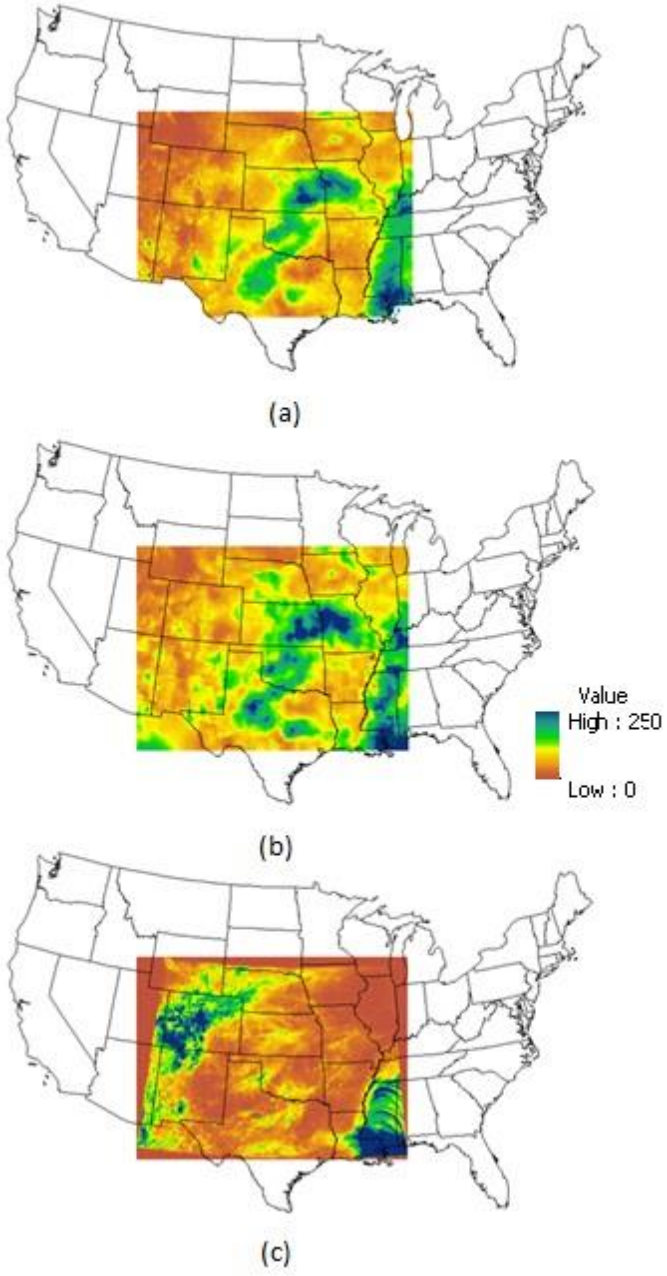

Figure 12. Monthly precipitation values for (a) PRISM, (b) METRIC-NLDAS and (c) WRF-CLM for August, 2005 (mm)

4.1.2. Comparison of 2007

2007 is a wet year for most of the region. Noah-MP without the option dynamic vegetation, bucket hydrology model with default vegetation option and bucket hydrology model with grass option are all evaluated and compared with METRIC ET results. Based on these results Noah-MP generates the closest ET results to METRIC. It can be concluded that for wet years Noah-MP is a good selection to calculate ET. Figures 13-20 show ET and precipitation products for 2007 May, June, July and August.

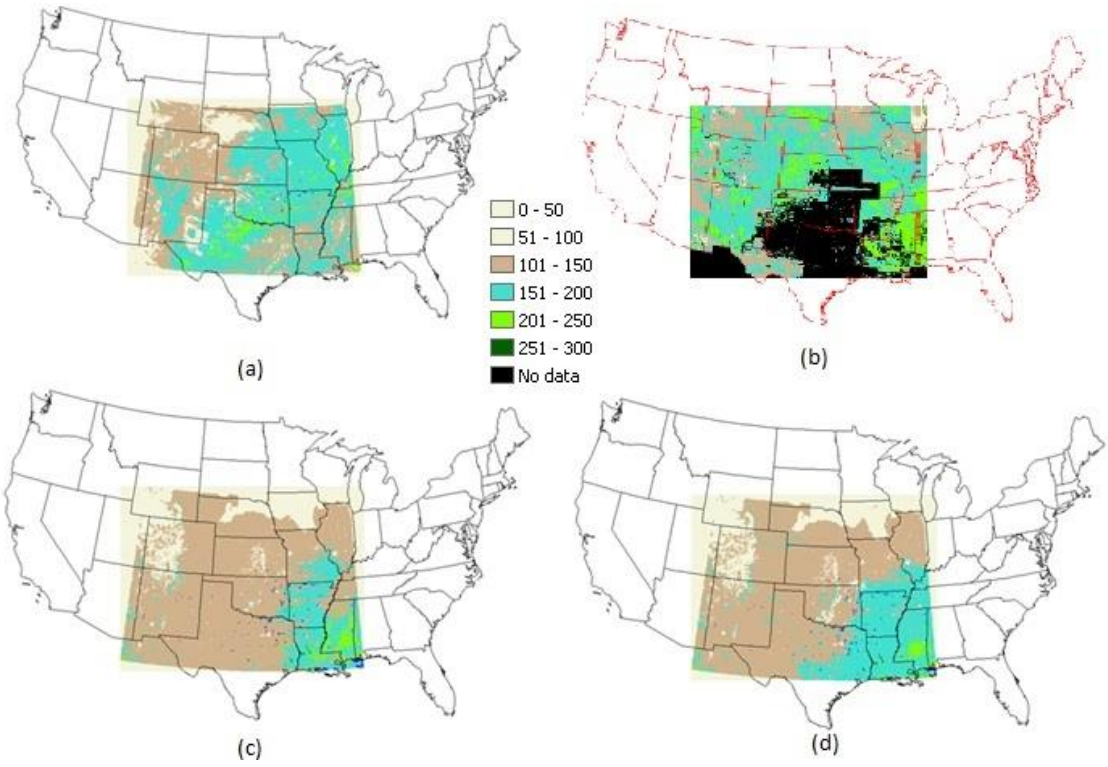

Figure 13. Monthly ET values for (a) Noah-MP, (b) METRIC, (c) BUCKET Default and (d) BUCKET Grass for May, 2007 (mm)

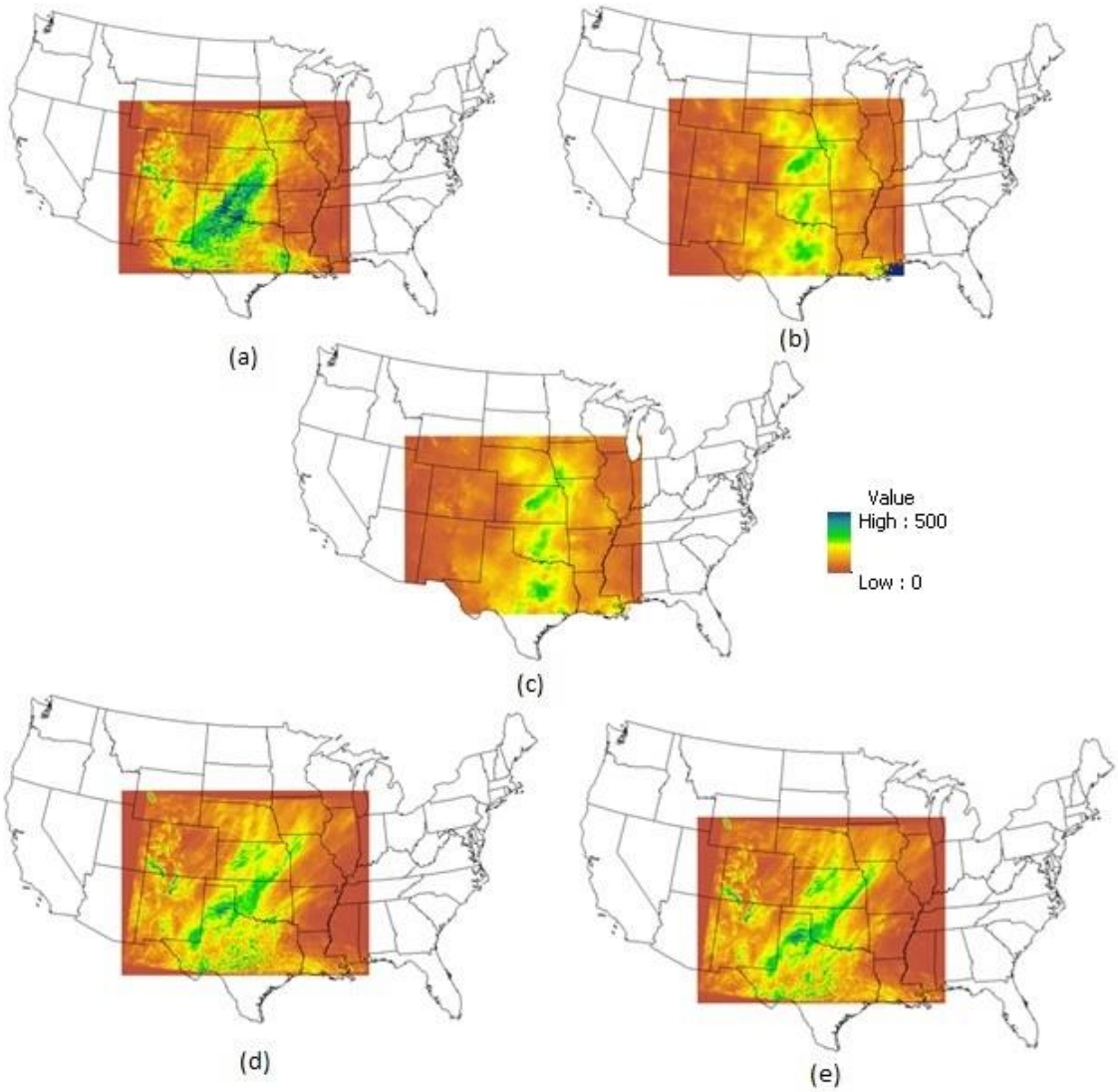

Figure 14. Monthly precipitation values for (a) Noah-MP, (b) METRIC-NLDAS, (c) PRISM, (d) BUCKET Default and (e) BUCKET Grass for May, 2007 (mm)

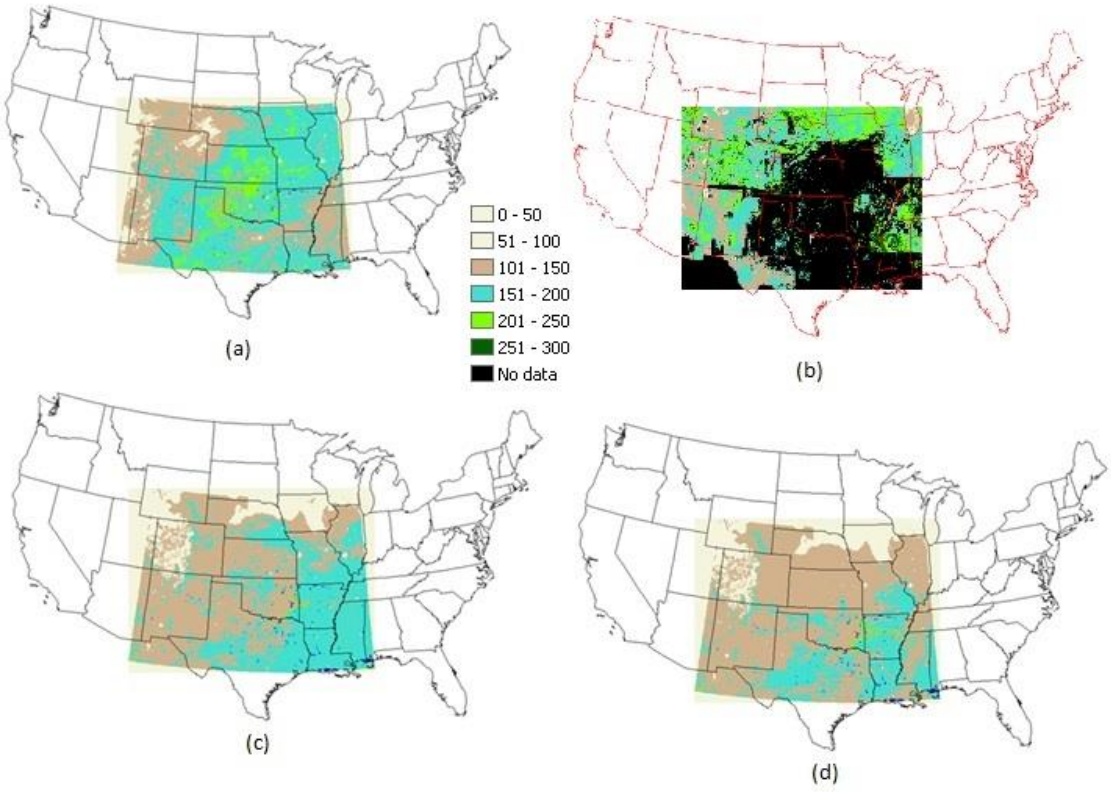

Figure 15. Monthly ET values for (a) Noah-MP, (b) METRIC, (c) BUCKET Default and (d) BUCKET Grass for June, 2007 (mm)

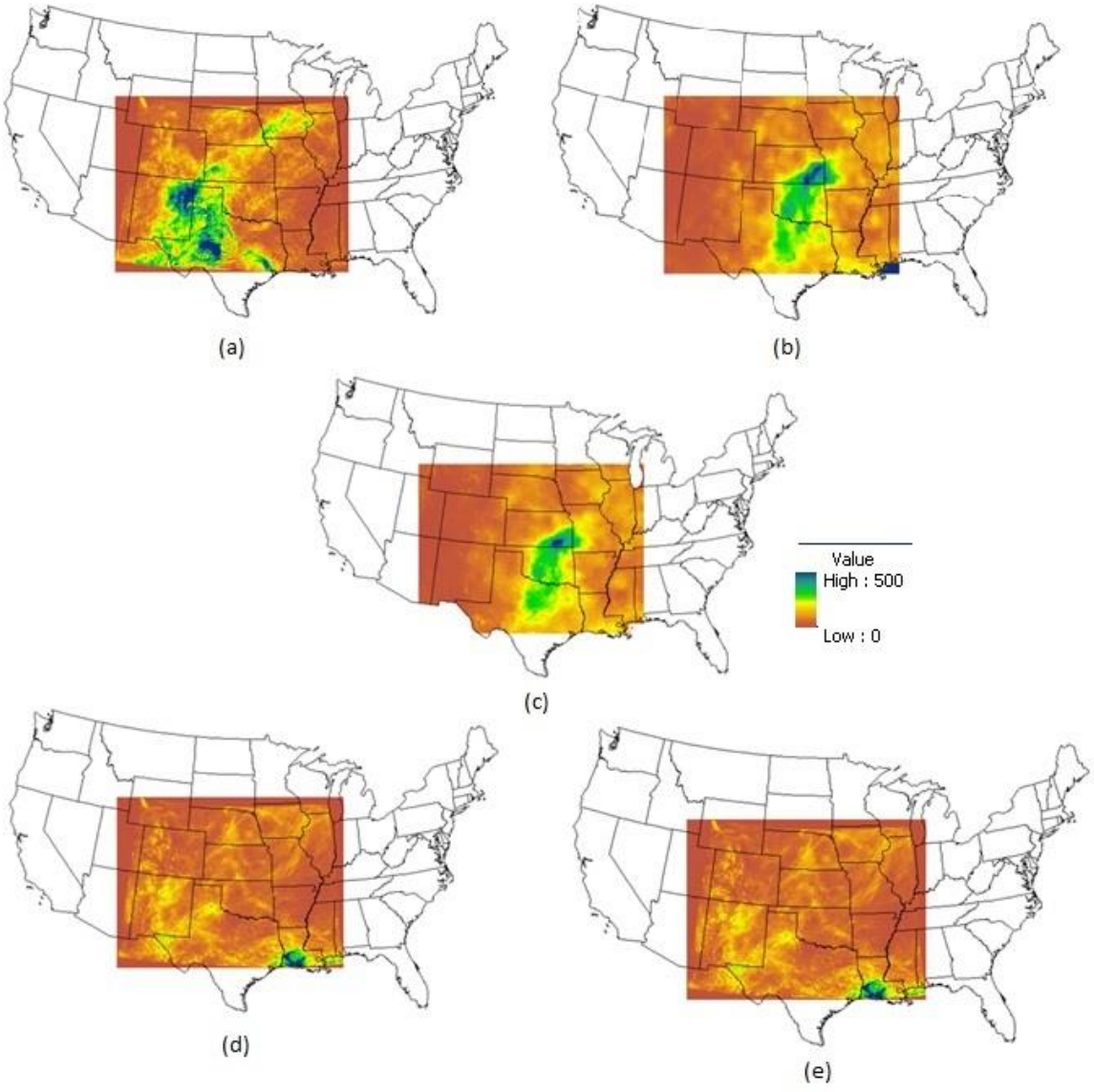

Figure 16. Monthly precipitation values for (a) Noah-MP, (b) METRIC-NLDAS, (c) PRISM, (d) BUCKET Default and (e) BUCKET Grass for June, 2007 (mm)

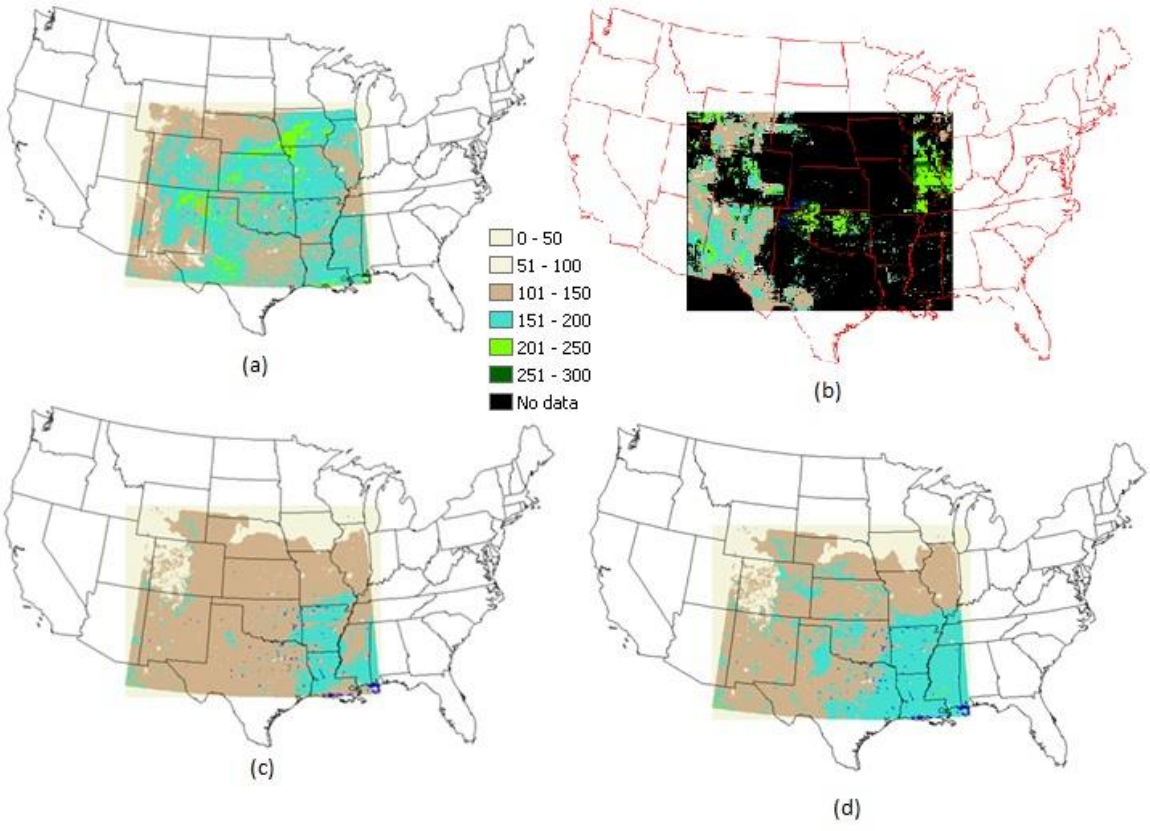

Figure 17. Monthly ET values for (a) Noah-MP, (b) METRIC, (c) BUCKET Default and (d) BUCKET Grass for July, 2007 (mm)

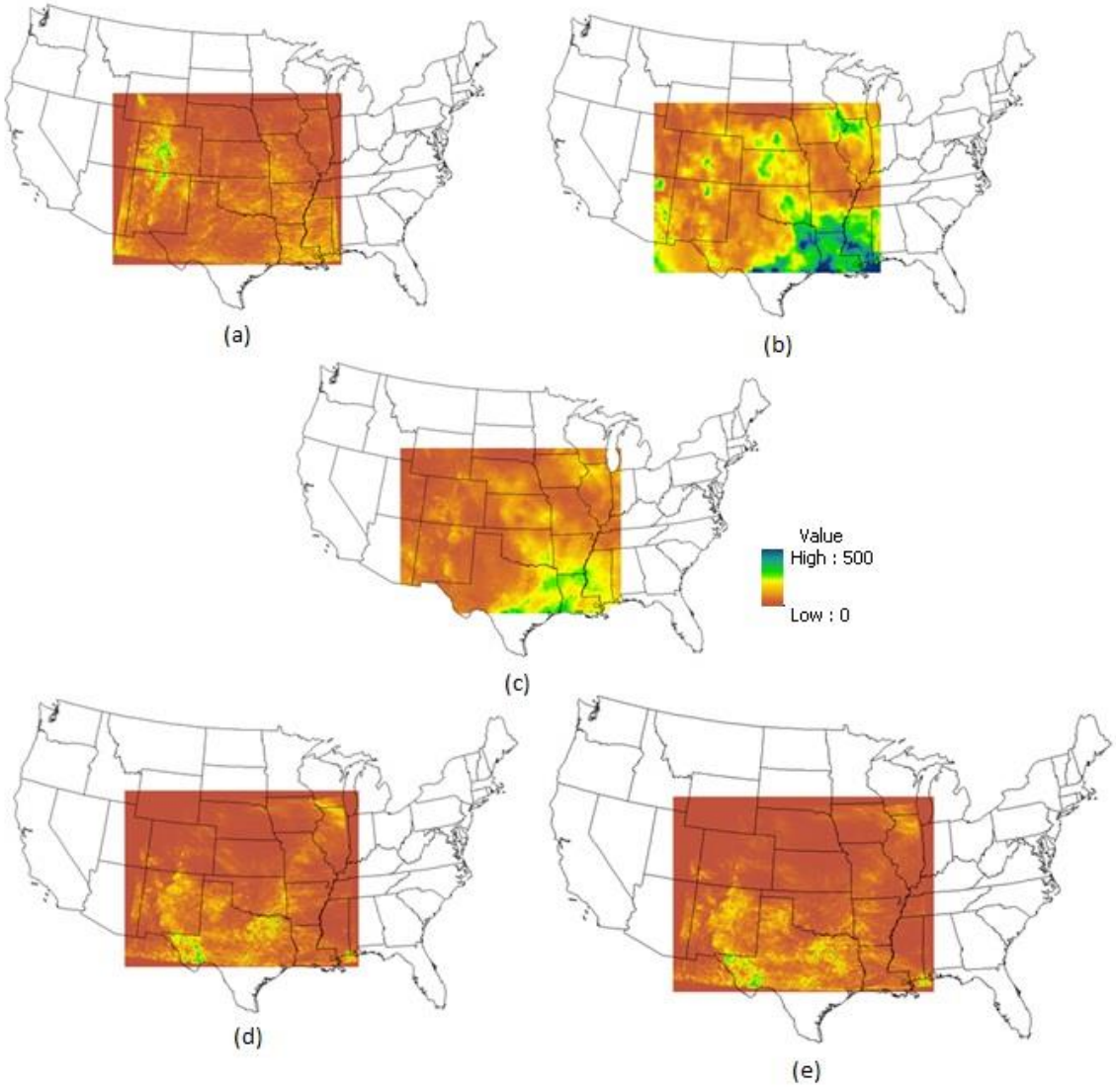

Figure 18. Monthly precipitation values for (a) Noah-MP, (b) METRIC-NLDAS, (c) PRISM, (d) BUCKET Default and (e) BUCKET Grass for July, 2007 (mm)

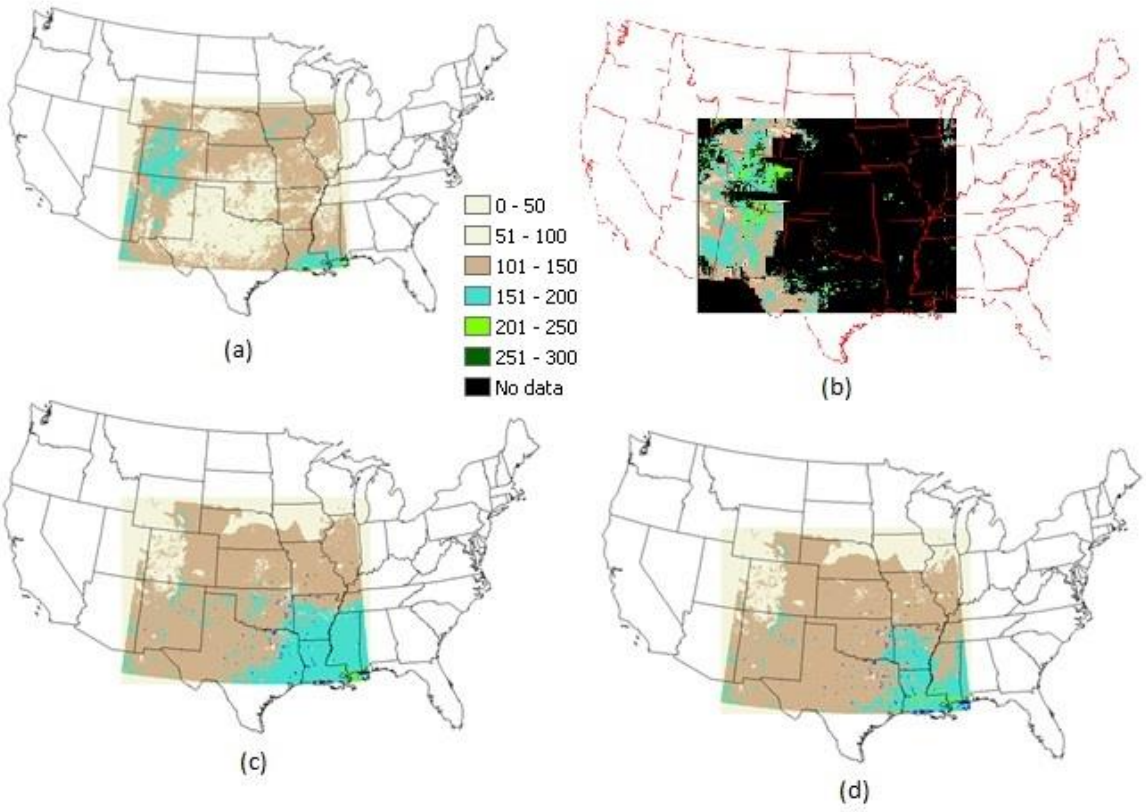

Figure 19. Monthly ET values for (a) Noah-MP, (b) METRIC, (c) BUCKET Default and (d) BUCKET Grass for August, 2007 (mm)

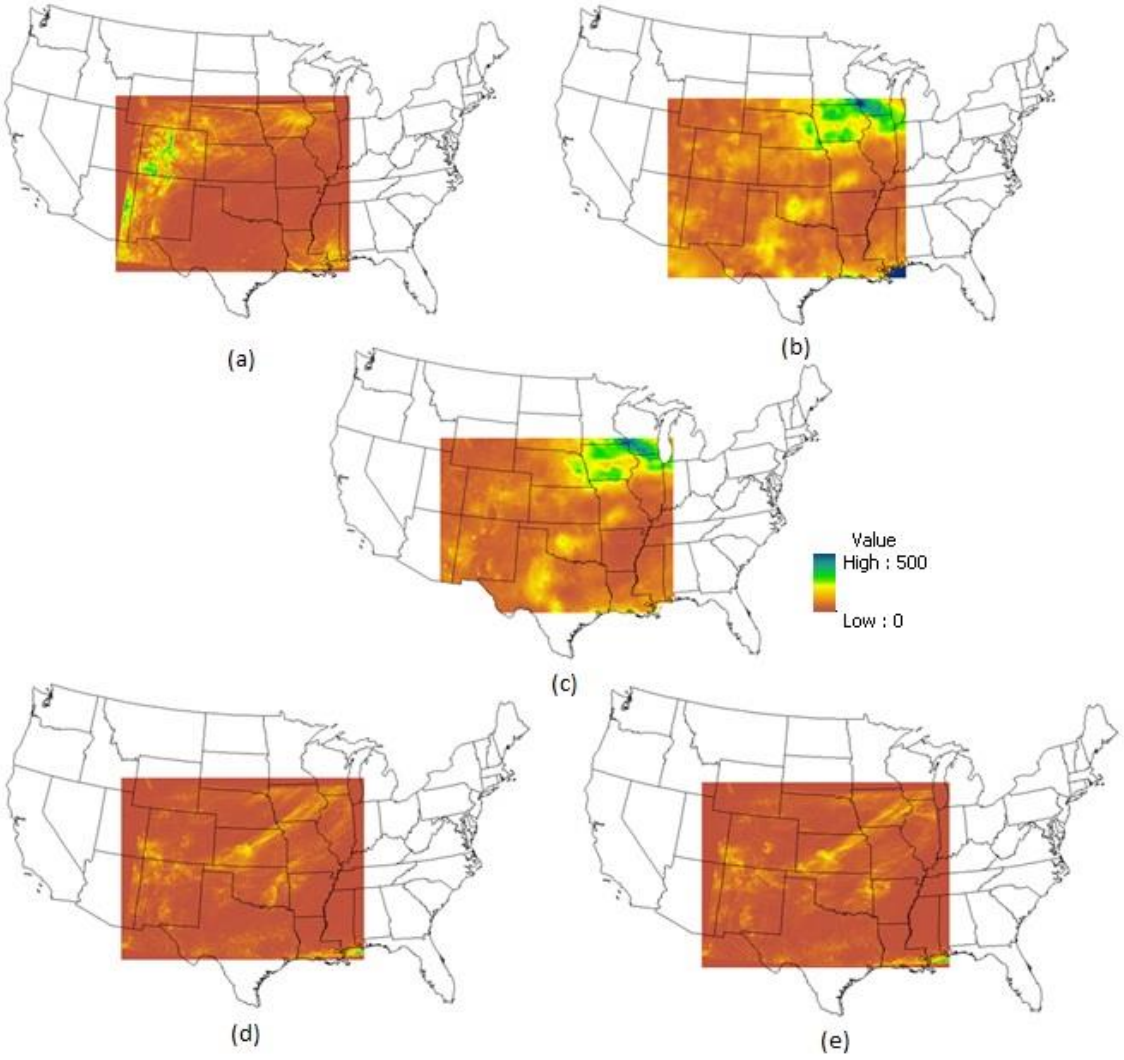

Figure 20. Monthly precipitation values for (a) Noah-MP, (b) METRIC-NLDAS, (c) PRISM, (d) BUCKET Default and (e) BUCKET Grass for August, 2007 (mm)

4.1.3. Comparison of 2012

Figure 21-28 shows ET and precipitation products for 2007 May, June, July and August.

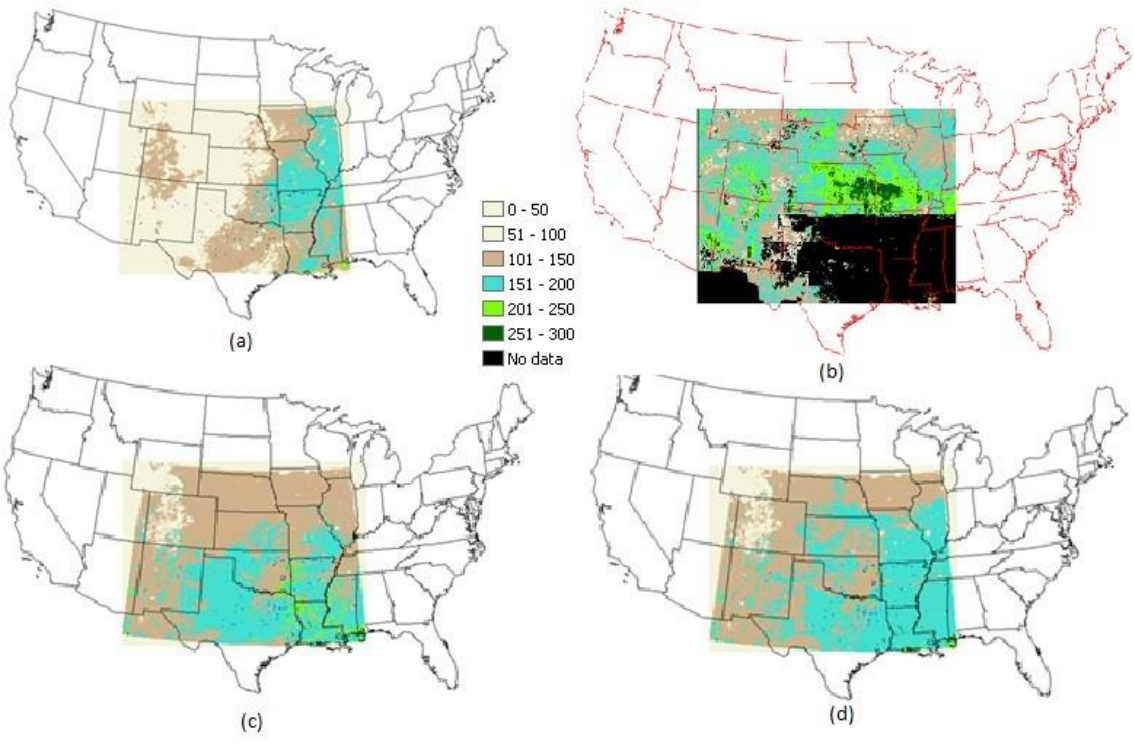

Figure 21. Monthly ET values for (a) Noah-MP, (b) METRIC, (c) BUCKET Default and (d) BUCKET Grass for May, 2012 (mm)

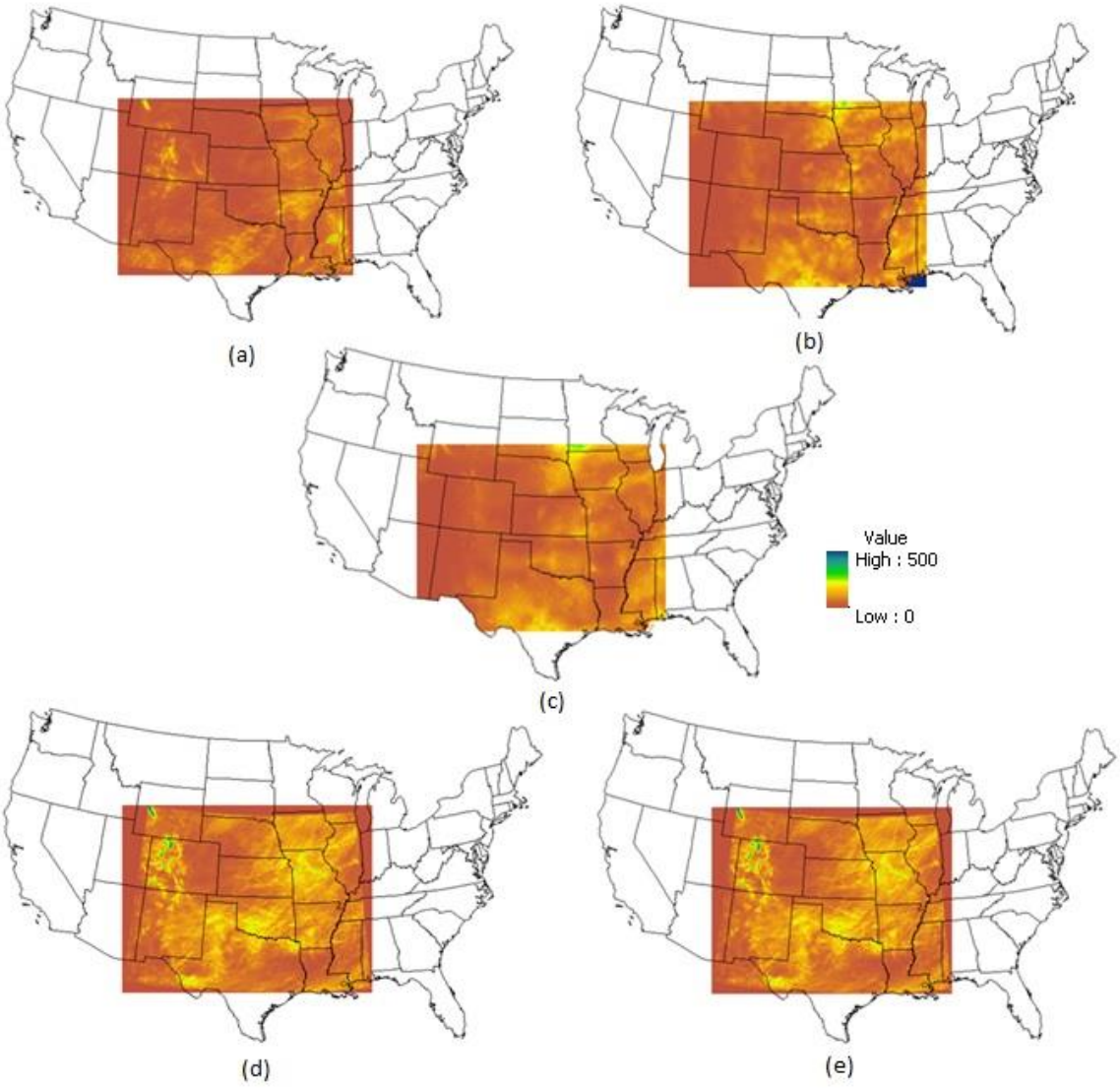

Figure 22. Monthly precipitation values for (a) Noah-MP, (b) METRIC-NLDAS, (c) PRISM, (d) BUCKET Default and (e) BUCKET Grass for May, 2012 (mm)

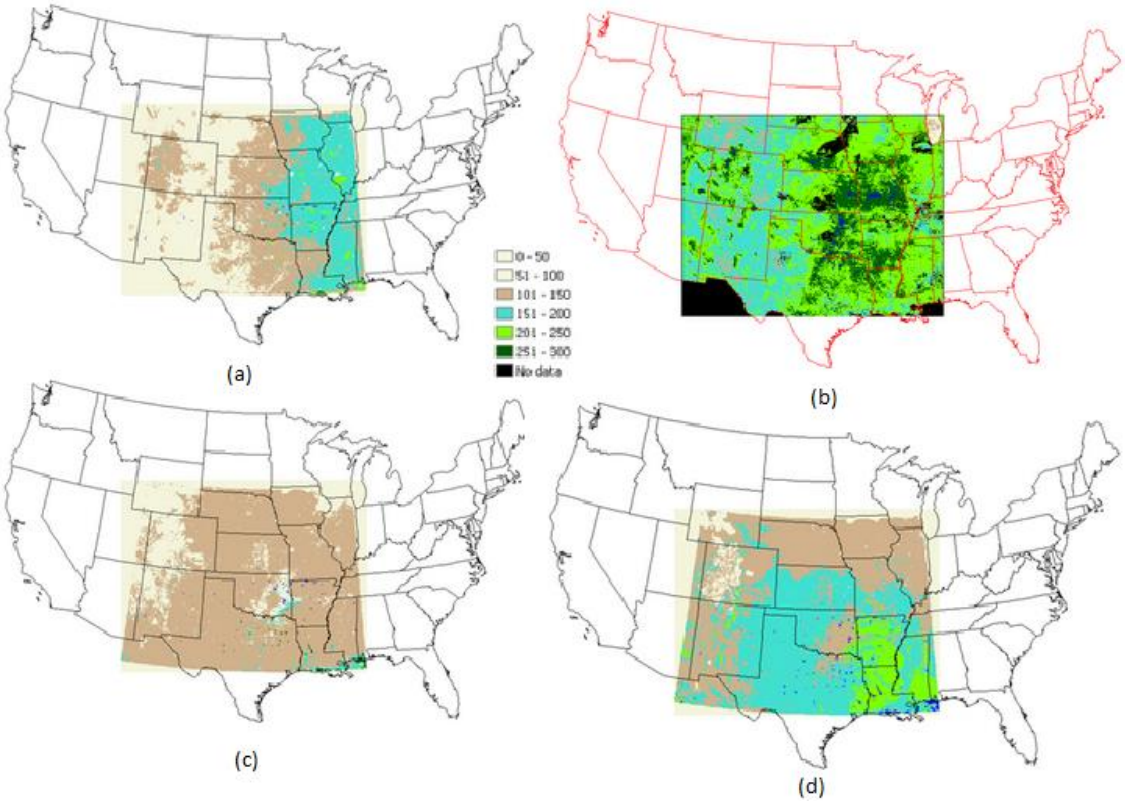

Figure 23. Monthly ET values for (a) Noah-MP, (b) METRIC, (c) BUCKET Default and (d) BUCKET Grass for June, 2012 (mm)

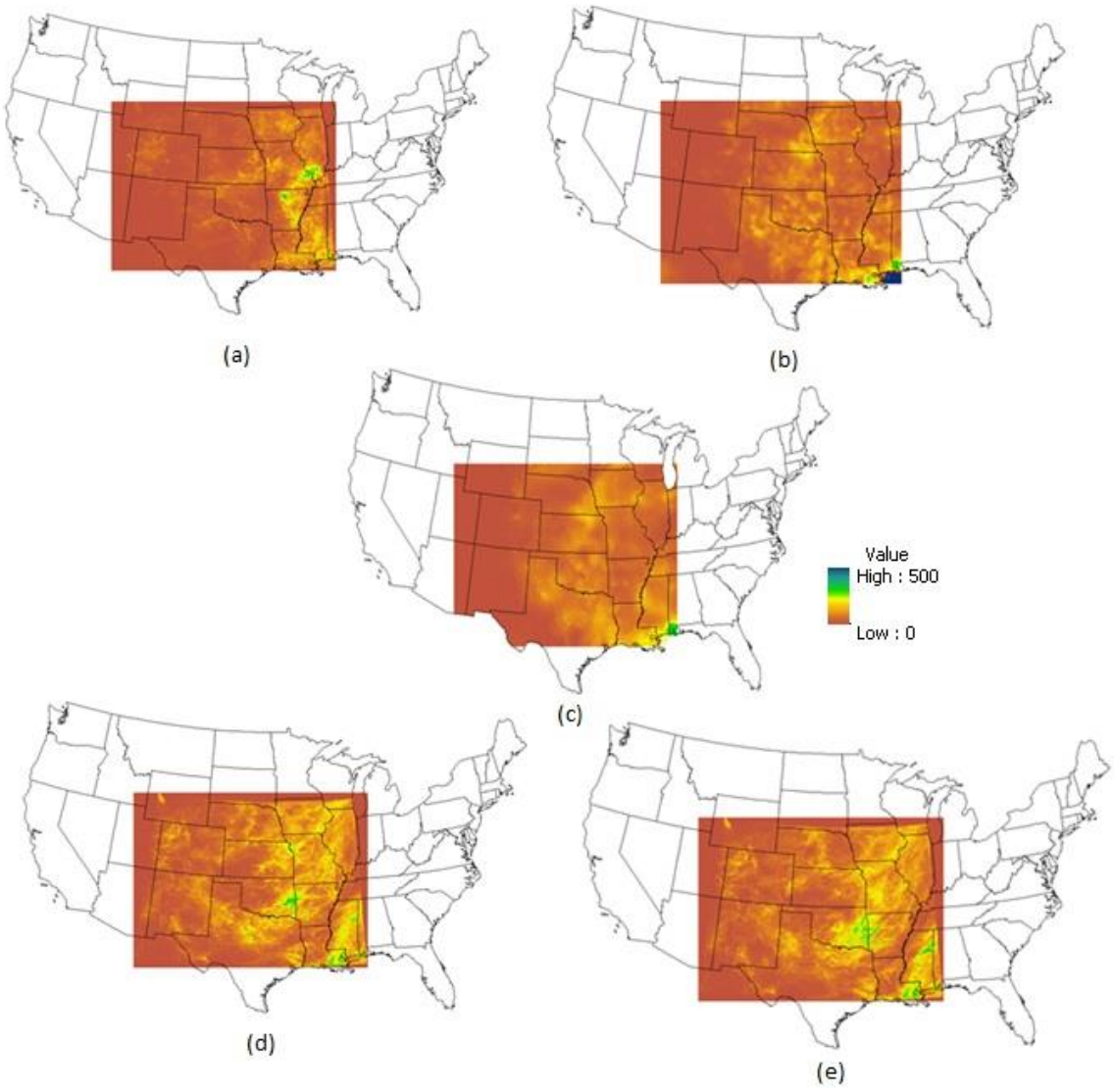

Figure 24. Monthly precipitation values for (a) Noah-MP, (b) METRIC-NLDAS, (c) PRISM, (d) BUCKET Default and (e) BUCKET Grass for June, 2012 (mm)

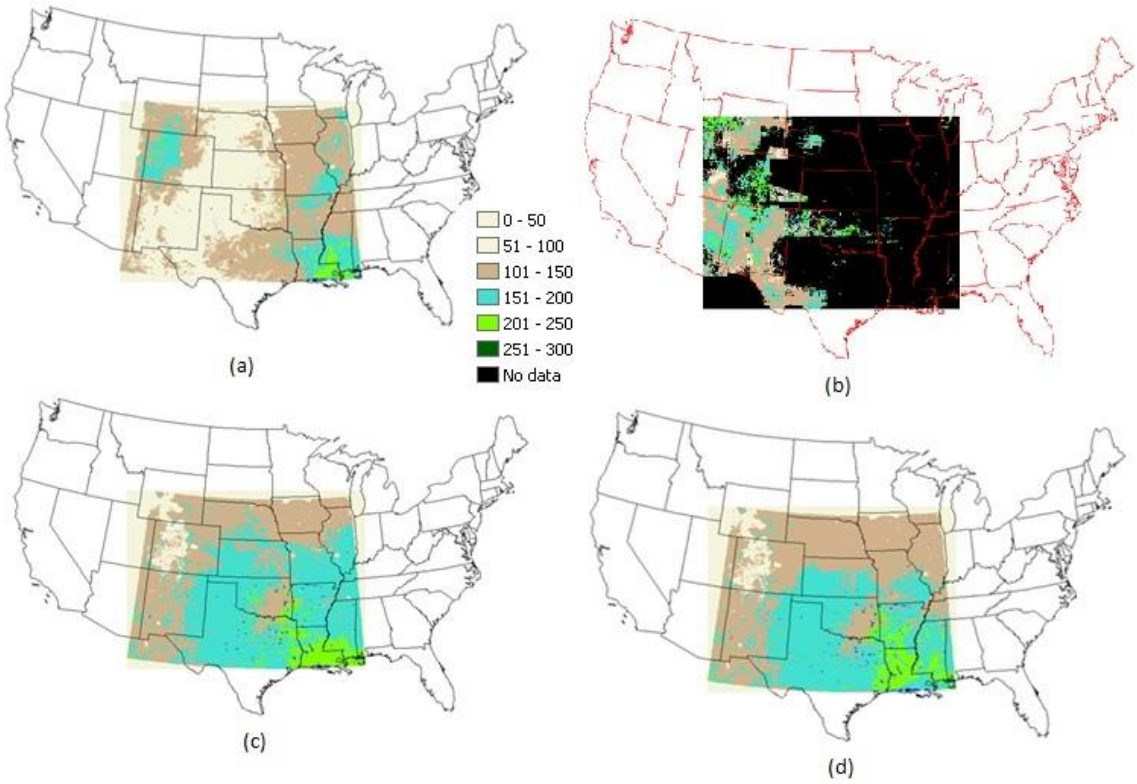

Figure 25. Monthly ET values for (a) Noah-MP, (b) METRIC, (c) BUCKET Default and (d) BUCKET Grass for July, 2012 (mm)

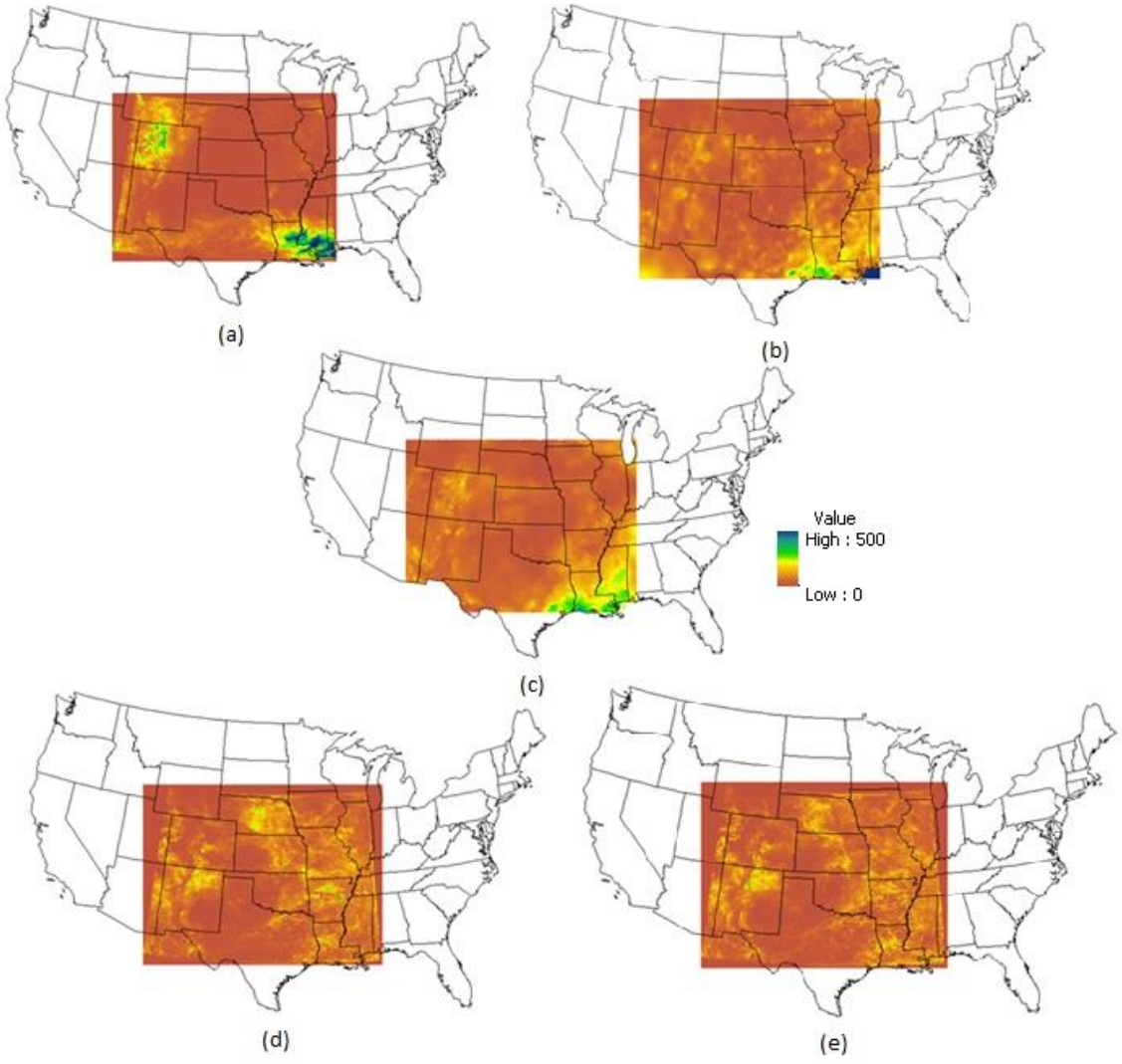

Figure 26. Monthly precipitation values for (a) Noah-MP, (b) METRIC-NLDAS, (c) PRISM, (d) BUCKET Default and (e) BUCKET Grass for July, 2012 (mm)

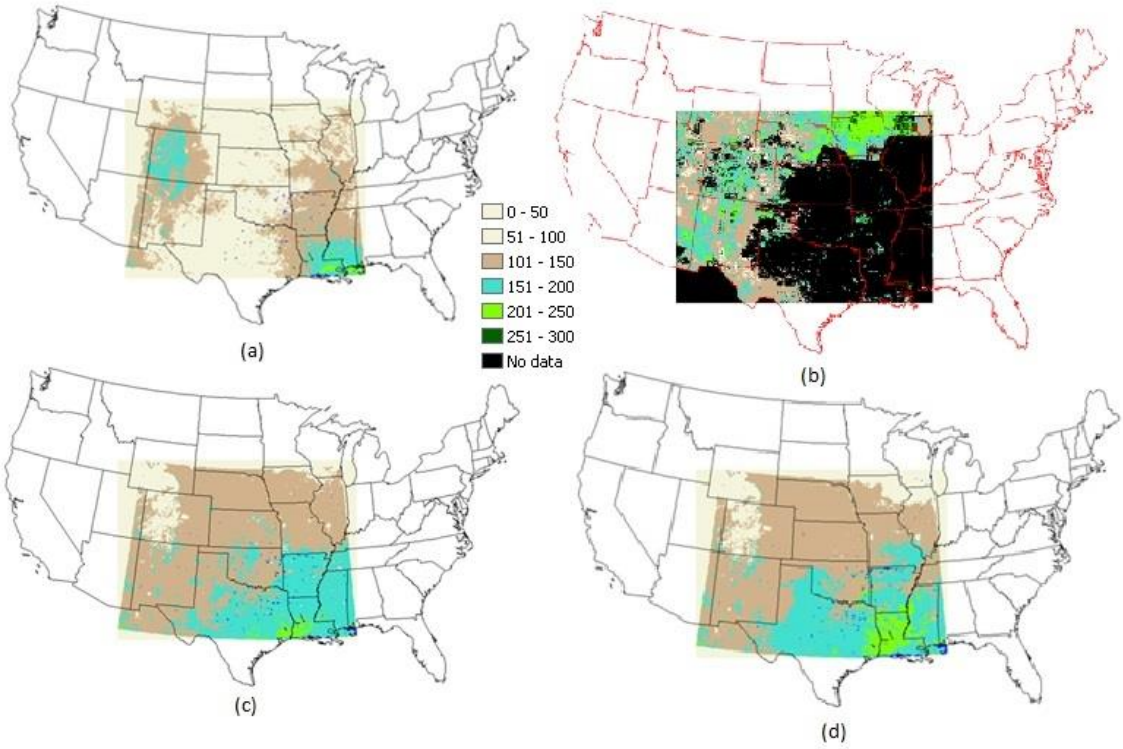

Figure 27. Monthly ET values for (a) Noah-MP, (b) METRIC, (c) BUCKET Default and (d) BUCKET Grass for August, 2012 (mm)

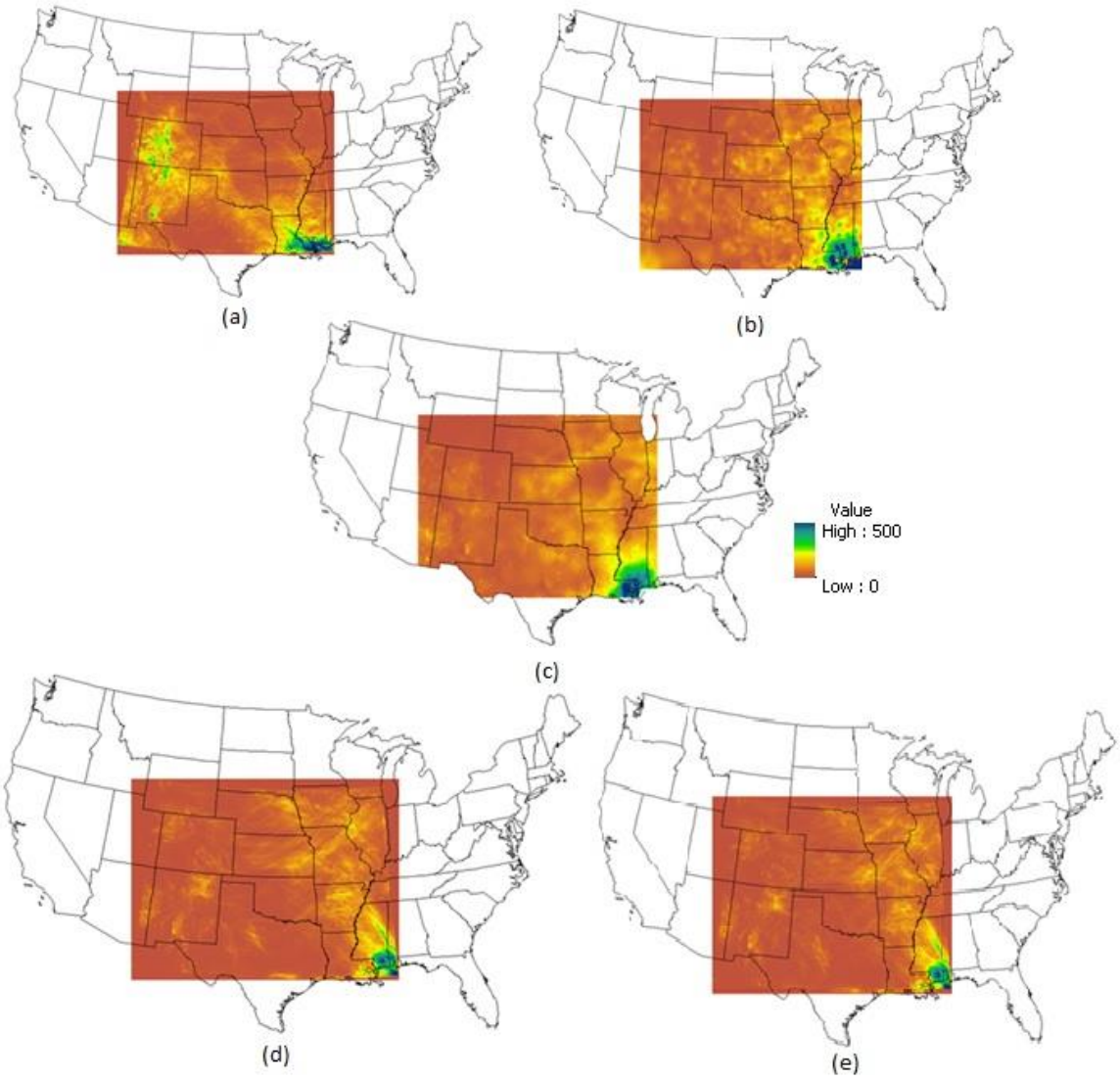

Figure 28. Monthly precipitation values for (a) Noah-MP, (b) METRIC-NLDAS, (c) PRISM, (d) BUCKET Default and (e) BUCKET Grass for August, 2012 (mm)

4.2. Statistical Evaluations

Among with the spatial comparisons, statistical evaluations are also conducted. Statistical analysis showed the differences in ET for different land use classes. The bar graphs in all figures are the mean values for every land use class in the x axis. The error bars are the standard errors. For the sake of clarity land use classes are given in number format, corresponding to the land use classes found in Table 1.

Tukey's pairwise test is used to indicate the significance level of different models. This test shows whether the differences of means for different groups are significant or not based on a confidence coefficient. This test was useful in this study since the difference between mean ET values for each land use class were analyzed with a systematic statistical method rather than visual observations. Tukey's analyses are conducted only for 2007 and 2012 runs, since for 2005 only comparison can be made between WRF-CLM and METRIC.

11	Open Water
12	Perennial Ice / Snow
21	Developed, Open Space
22	Developed, Low Intensity
23	Developed, Medium Intensity
24	Developed, High Intensity
31	Barren Land (Rock / Sand / Clay)
41	Deciduous Forest
42	Evergreen Forest
43	Mixed Forest
51	Dwarf Scrub
52	Shrub / Scrub
71	Grassland / Herbaceous
72	Sedge / Herbaceous
73	Lichens
74	Moss
81	Pasture / Hay
82	Cultivated Crops
90	Woody Wetlands
95	Emergent Herbaceous Wetlands

Table 1. Explanations of the land use codes.

4.2.1. Comparison for 2005

For the 2005, CLM is coupled with WRF model is compared with METRIC. Both ET and precipitation results are compared to observe the spatial patterns between models. In all graphics, the colored bars are the mean ET values for the given month and given land use class. Error bars are the standard error values. Mean ET values for each land use class is taken due to the fact that pixel by pixel comparison complicates the visualizations.

First consideration about the underestimation of ET by WRF-CLM could be the irrigation effect. Lack of irrigation in the model can result in low soil moisture content, which in turn results in low ET results for the agricultural areas. This can cause different consequences among the results such as changing the precipitation, temperature and even wind speed for the next days. Figure 30-37 shows ET and precipitation statistical comparison products for 2005 May, June, July and August.

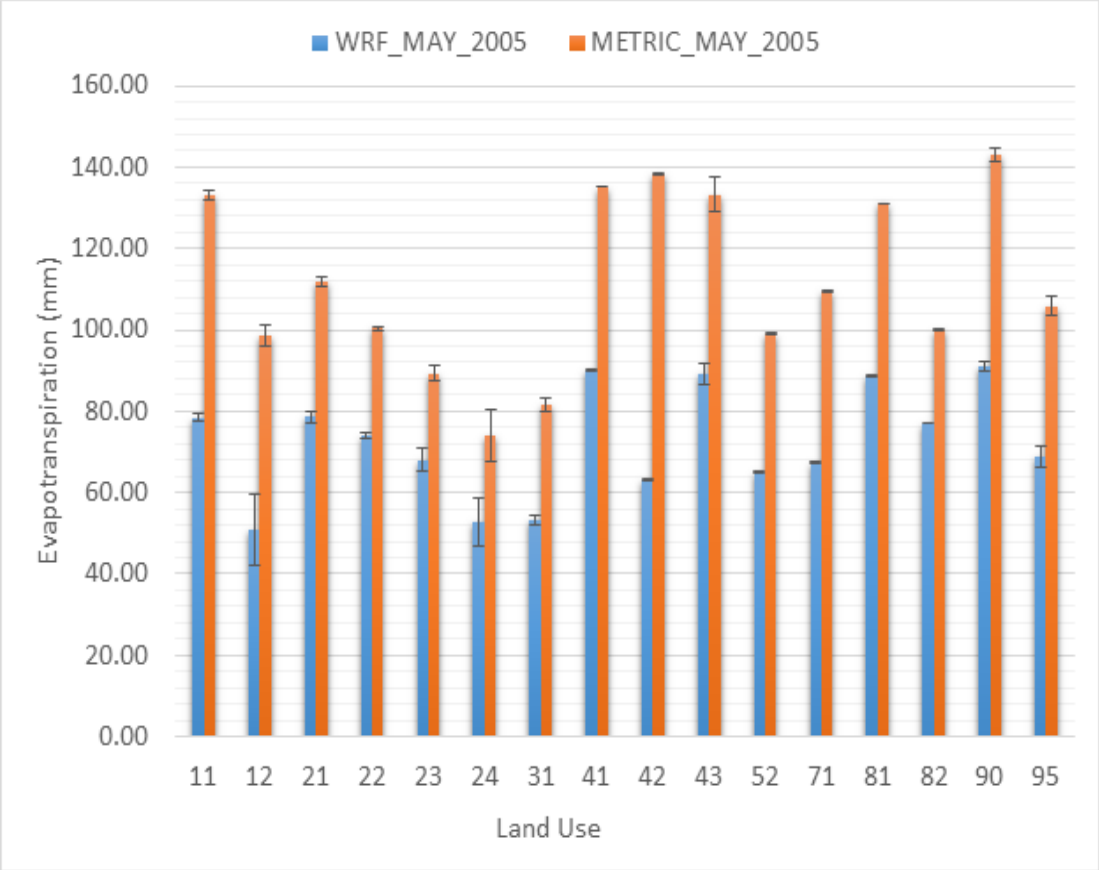

Figure 29. METRIC vs WRF-CLM Mean Evapotranspiration for May, 2005

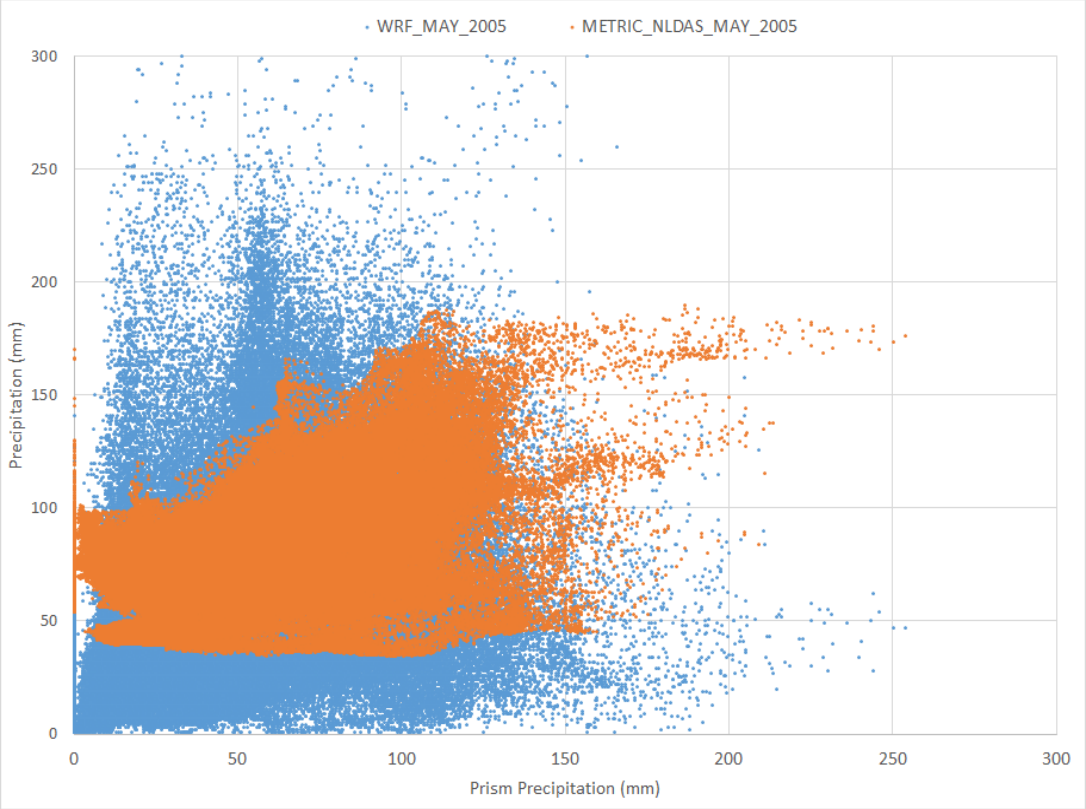

Figure 30. Comparison of WRF-CLM precipitation product and METRIC-NLDAS precipitation product against PRISM data in the x axis for May, 2005

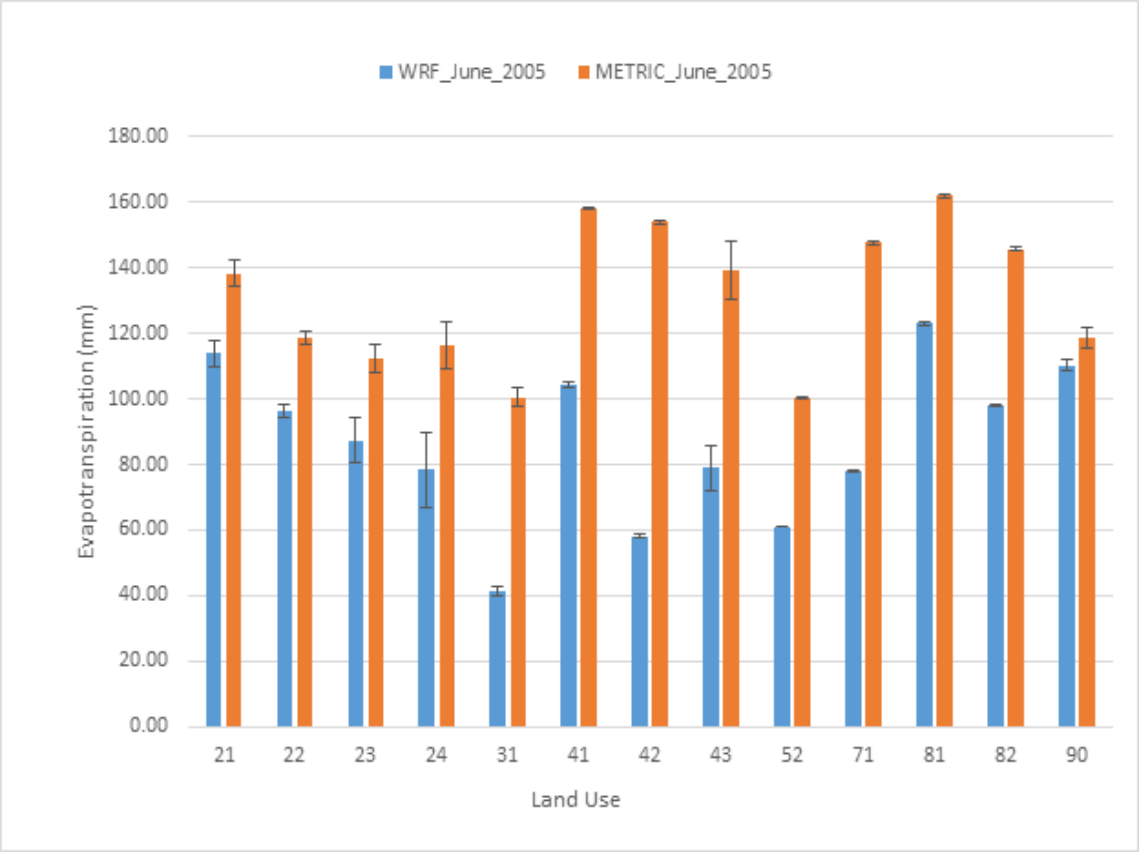

Figure 31. METRIC vs WRF-CLM Mean Evapotranspiration for June, 2005

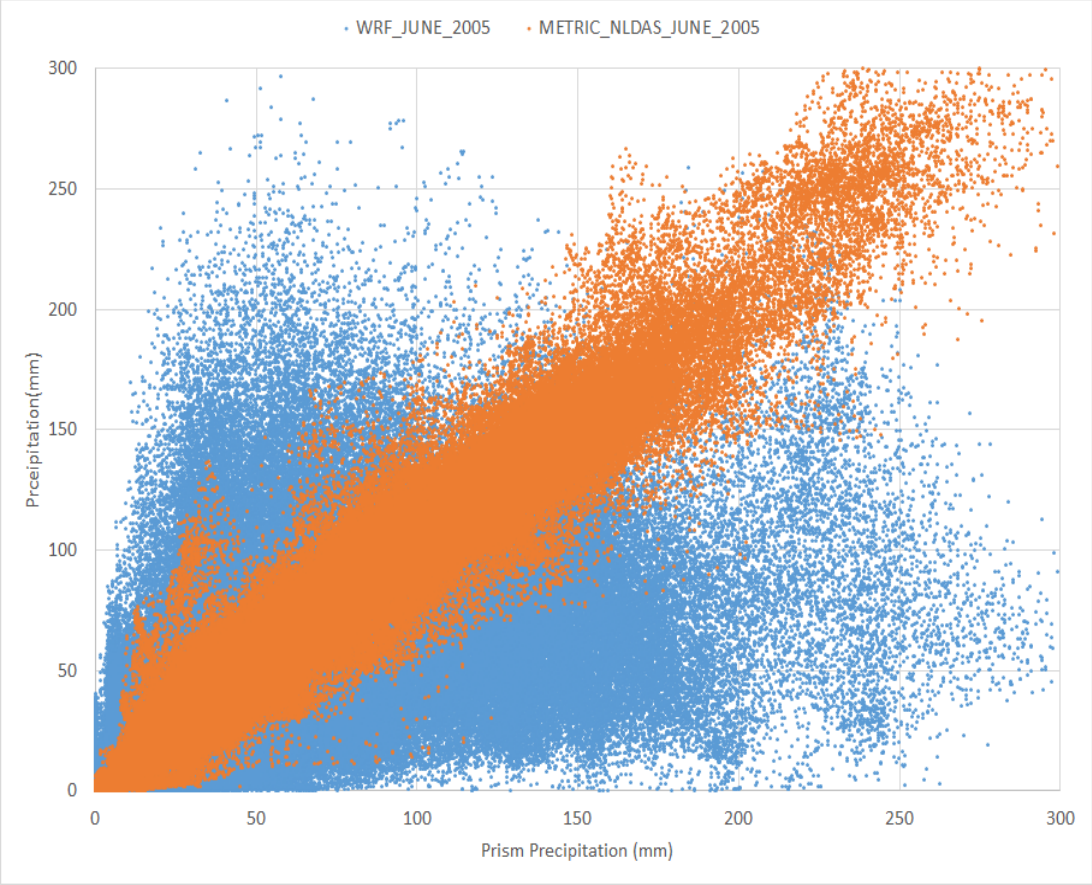

Figure 32. Comparison of WRF-CLM precipitation product and METRIC-NLDAS precipitation product against PRISM data in the x axis for June, 2005

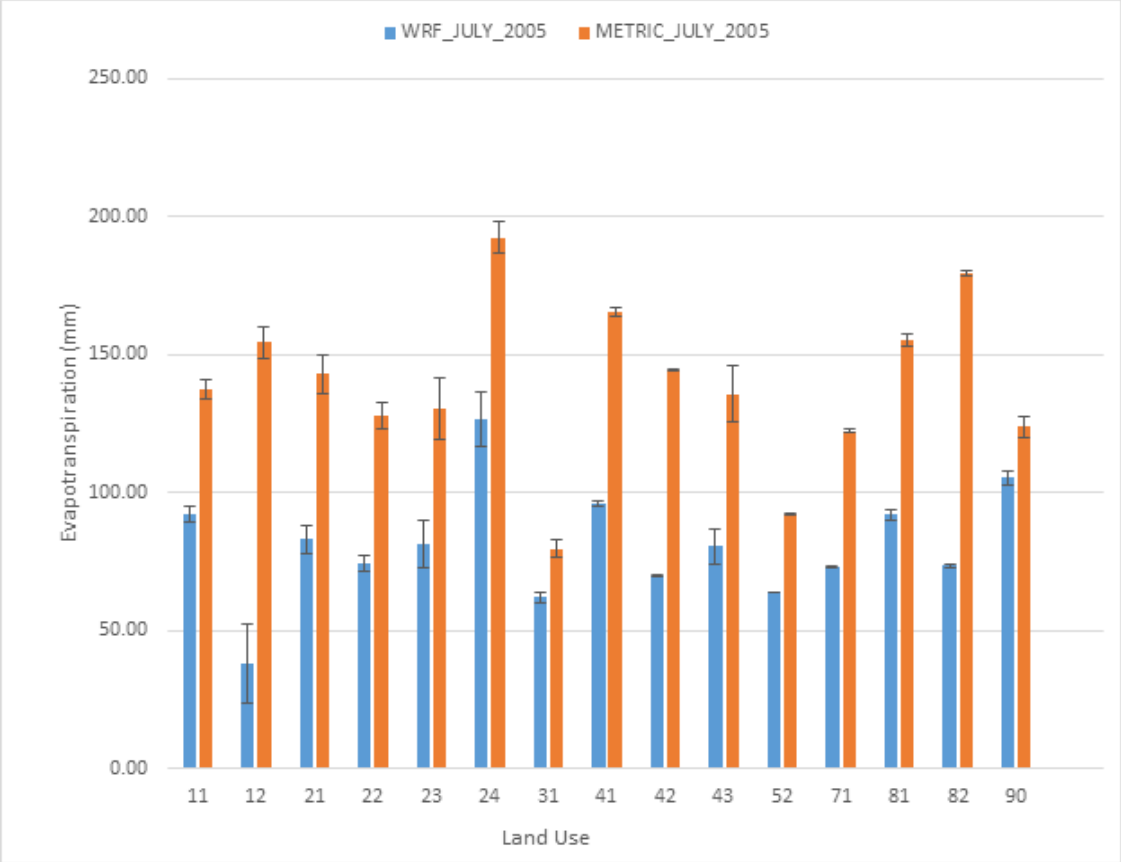

Figure 33. METRIC vs WRF-CLM Mean Evapotranspiration for July, 2005

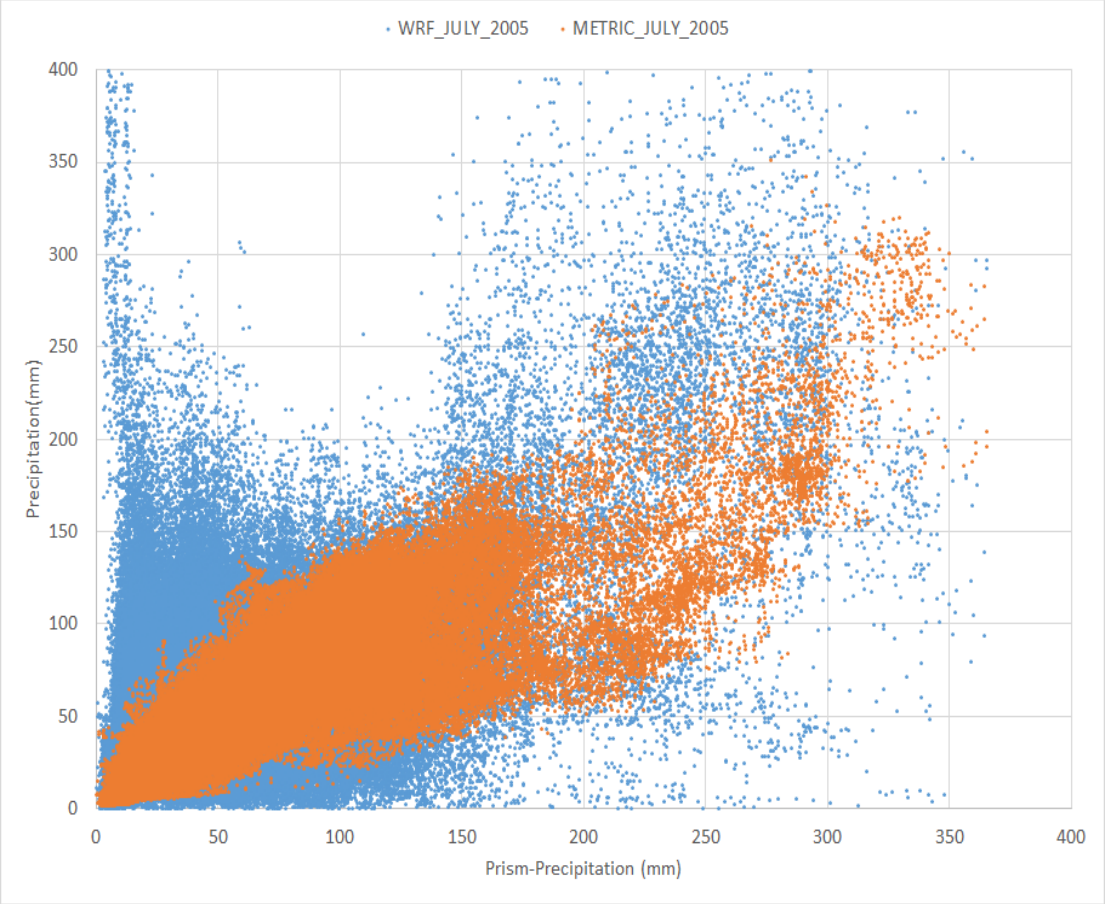

Figure 34. Comparison of WRF-CLM precipitation product and METRIC-NLDAS precipitation product against PRISM data in the x axis for July, 2005

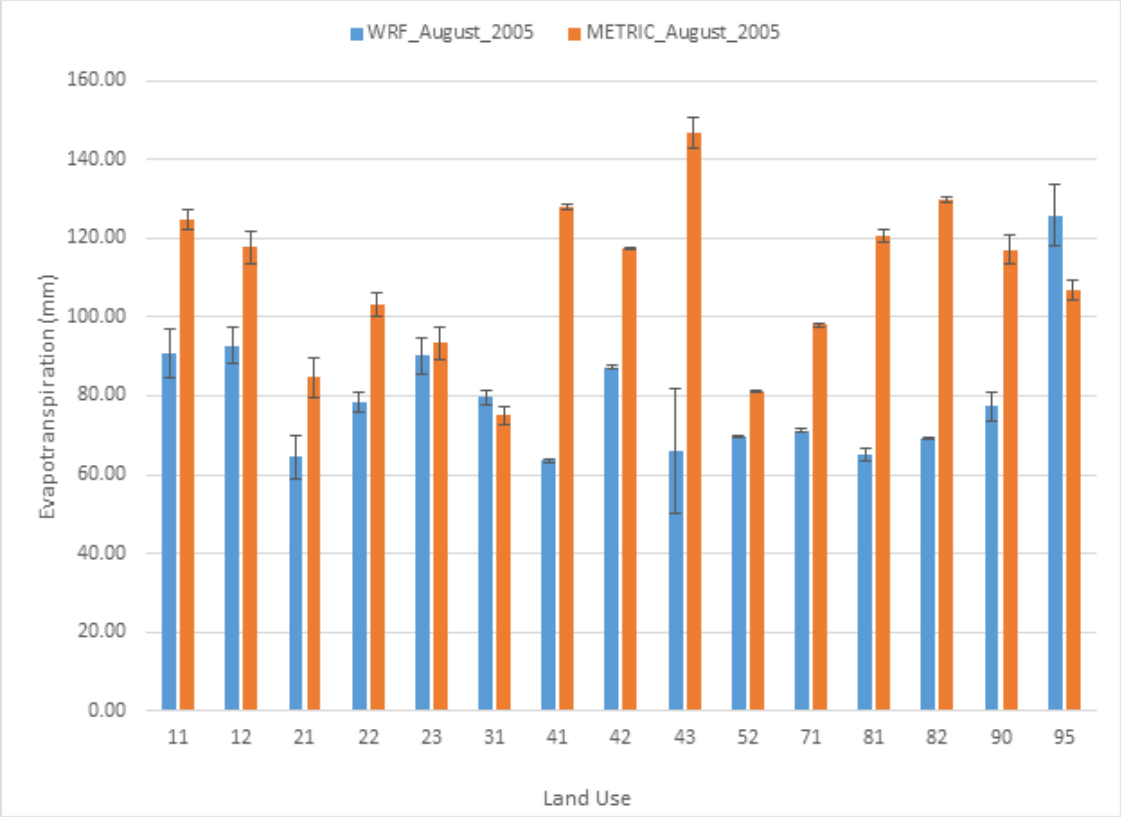

Figure 35. METRIC vs WRF-CLM Mean Evapotranspiration for August, 2005

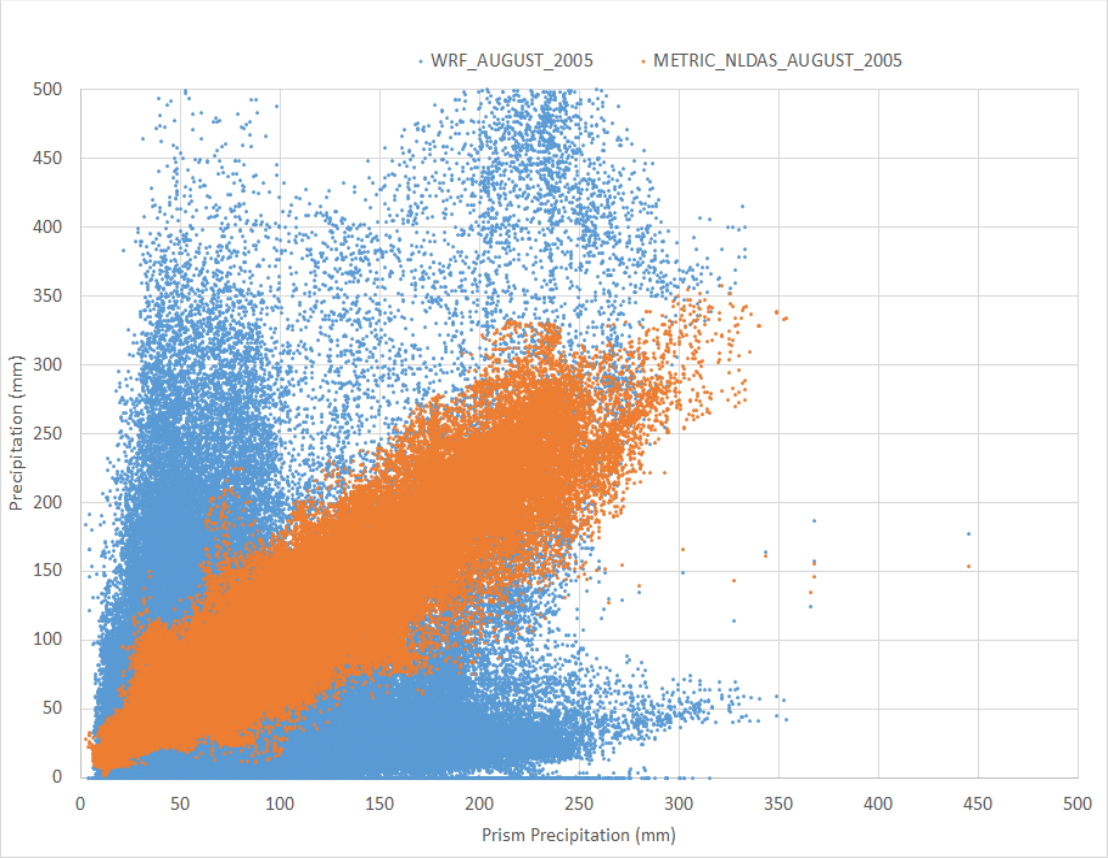

Figure 36. Comparison of WRF-CLM precipitation product and METRIC-NLDAS precipitation product against PRISM data in the x axis for August, 2005

4.2.2. Comparison of 2007

Almost all the models are significantly different than METRIC towards underestimation. This is a systematic bias in the WRF dataset. WRF ET datasets resembles the WRF precipitation datasets since there is no irrigation parameter in WRF, which is almost half of the water input to the system with precipitation. Figure 38-41 shows ET and precipitation statistical comparison products for 2007 May, June, July and August.

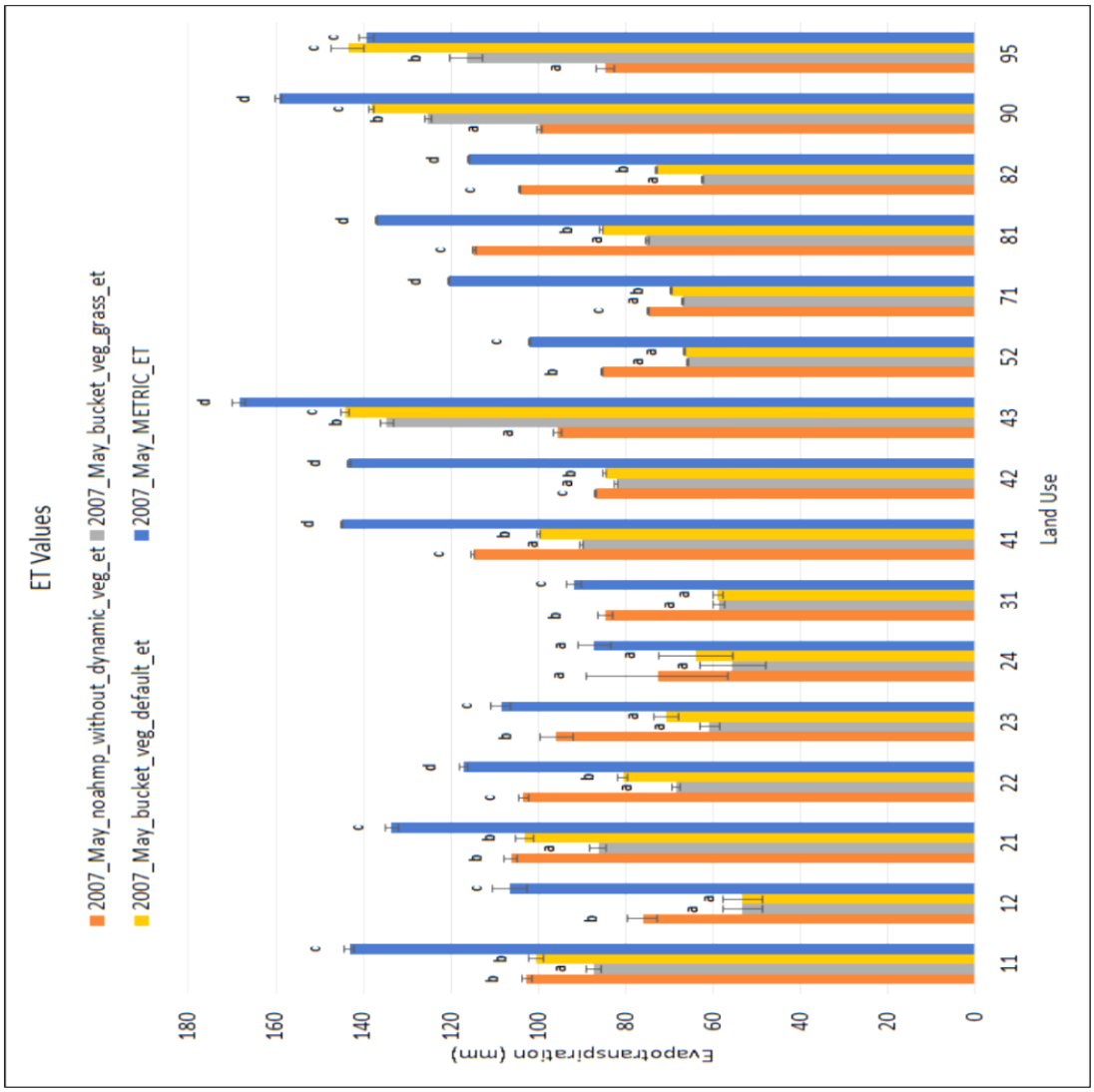

Figure 37. ET values for METRIC and different land surface models coupled with WRF for May, 2007

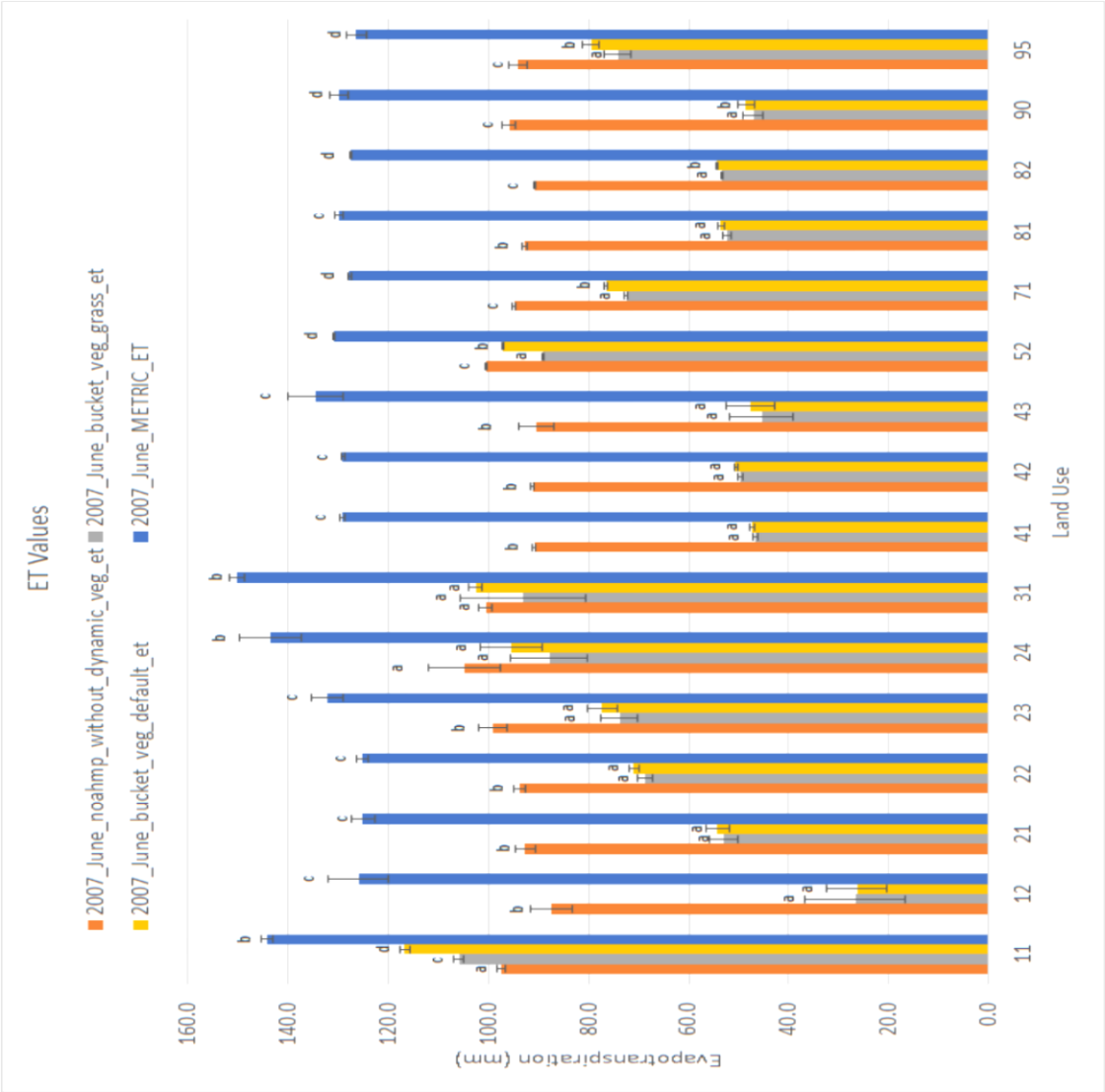

Figure 38. ET values for METRIC and different land surface models coupled with WRF for June, 2007

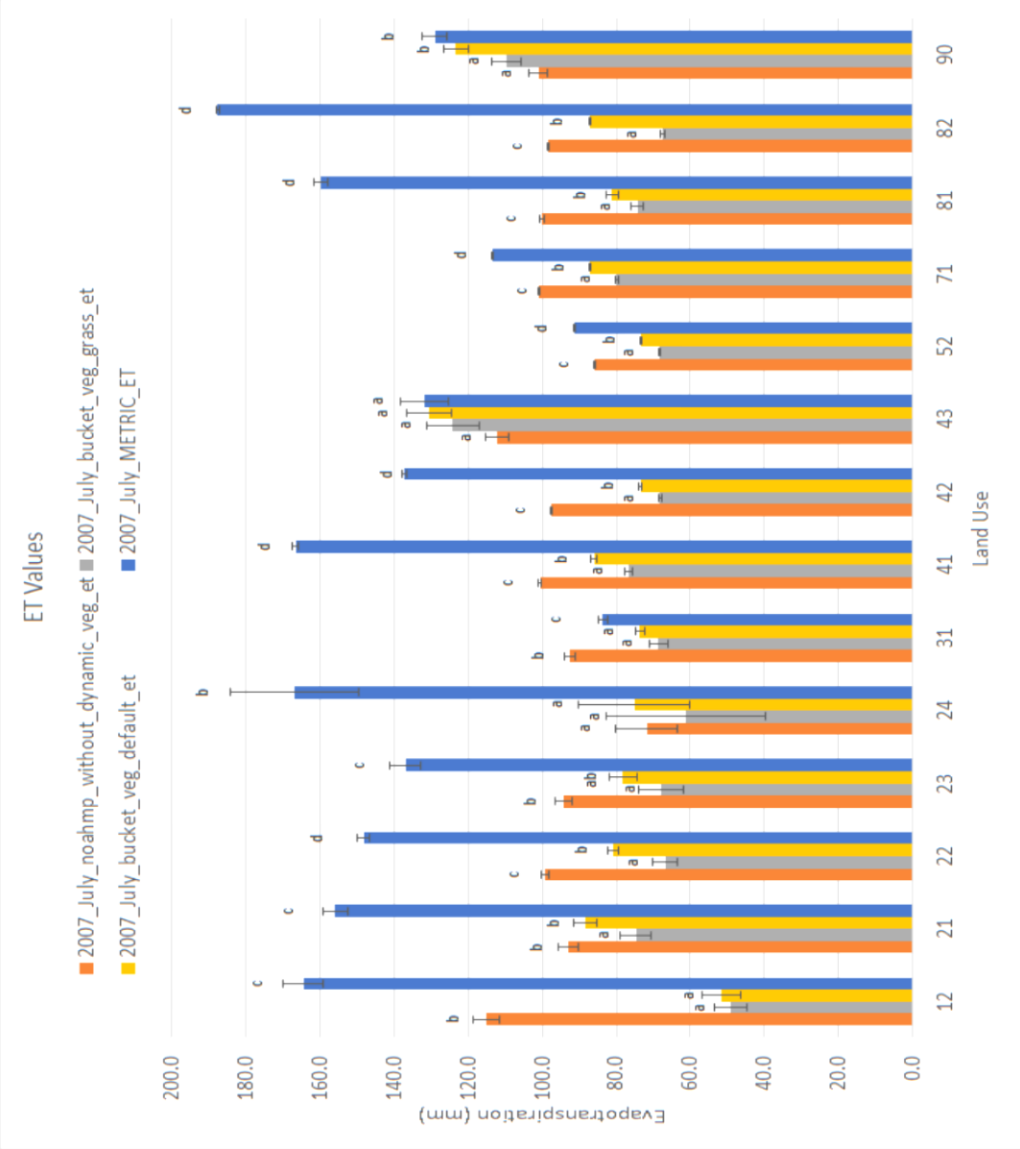

Figure 39. ET values for METRIC and different land surface models coupled with WRF for July, 2007

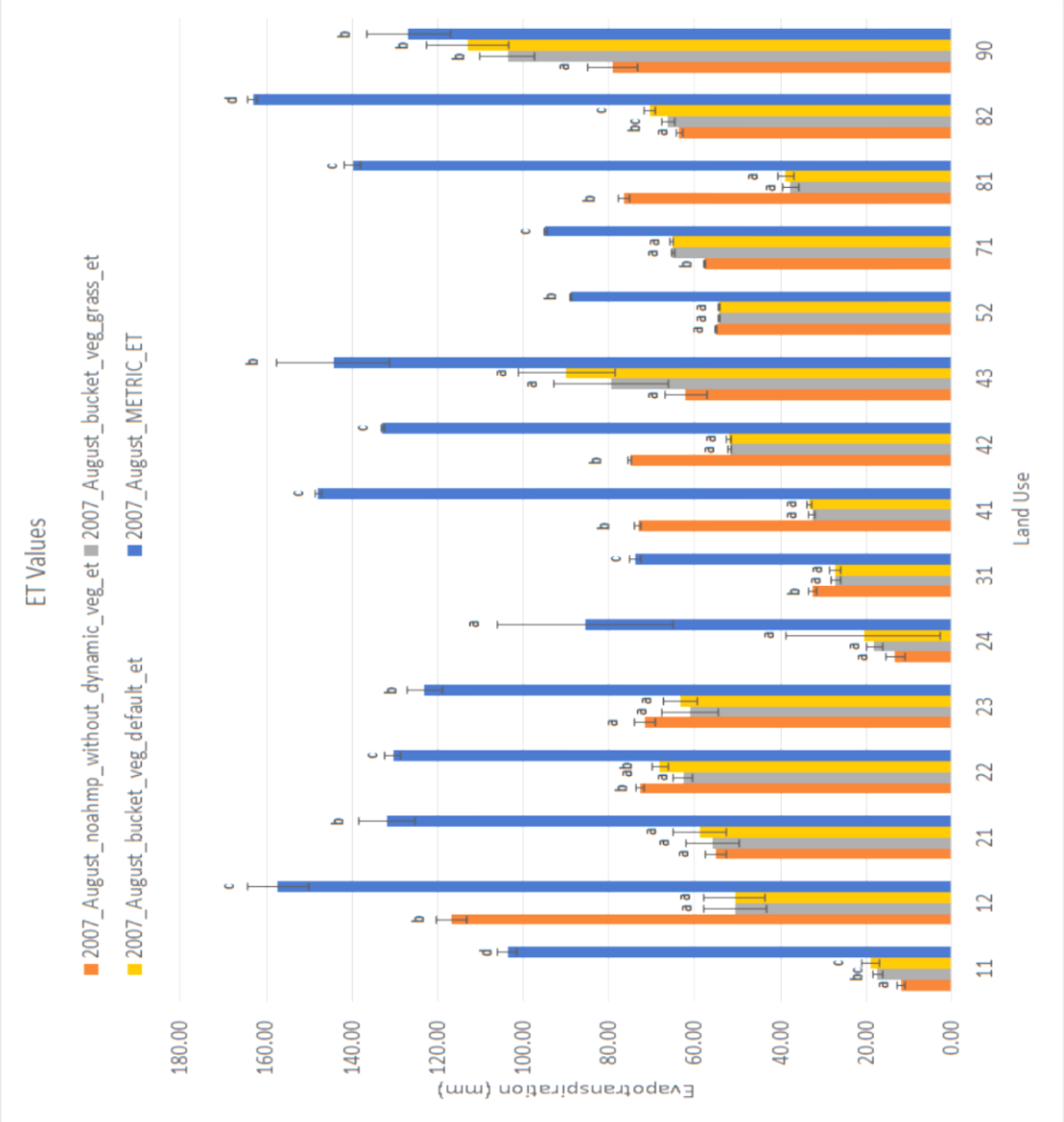

Figure 40. ET values for METRIC and different land surface models coupled with WRF for August, 2007

4.2.3. Comparison of 2012

Since 2012 is a dry year, mean values were reduced for all models since drought reduces ET. During this year Bucket models have a better accuracy than the Noah-MP. Figure 42-45 shows ET and precipitation statistical comparison products for 2012 May, June, July and August.

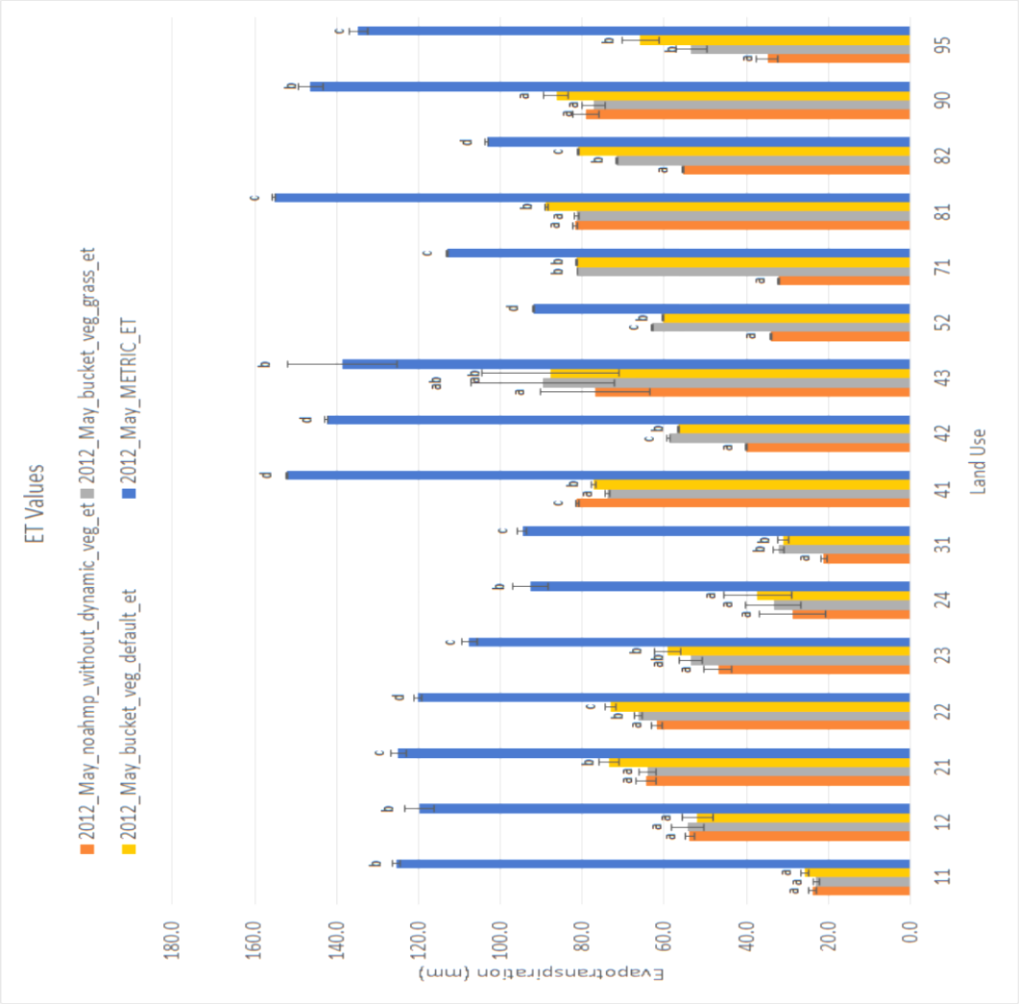

Figure 41. ET values for METRIC and different land surface models coupled with WRF for May, 2012

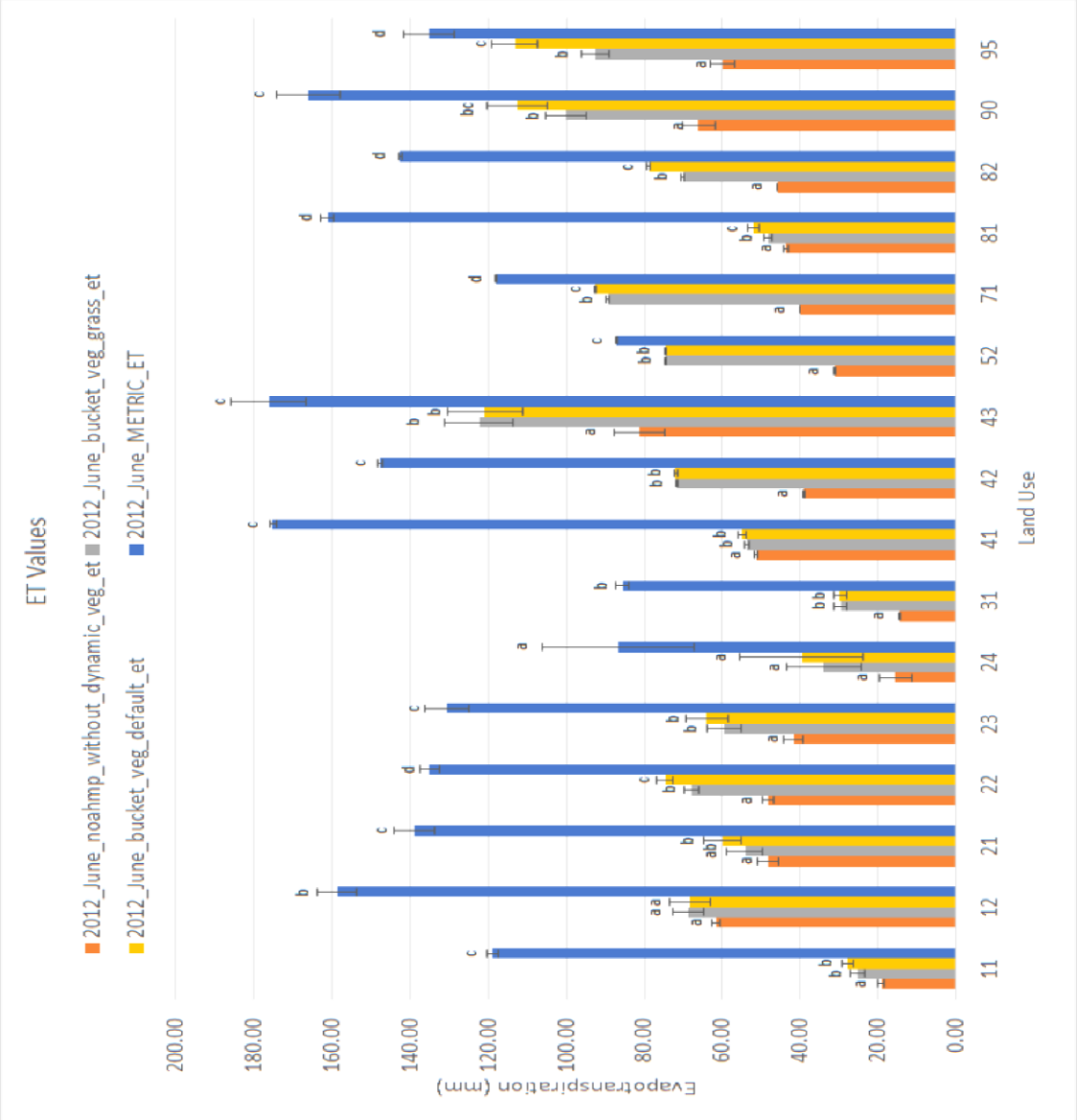

Figure 42. ET values for METRIC and different land surface models coupled with WRF for June, 2012

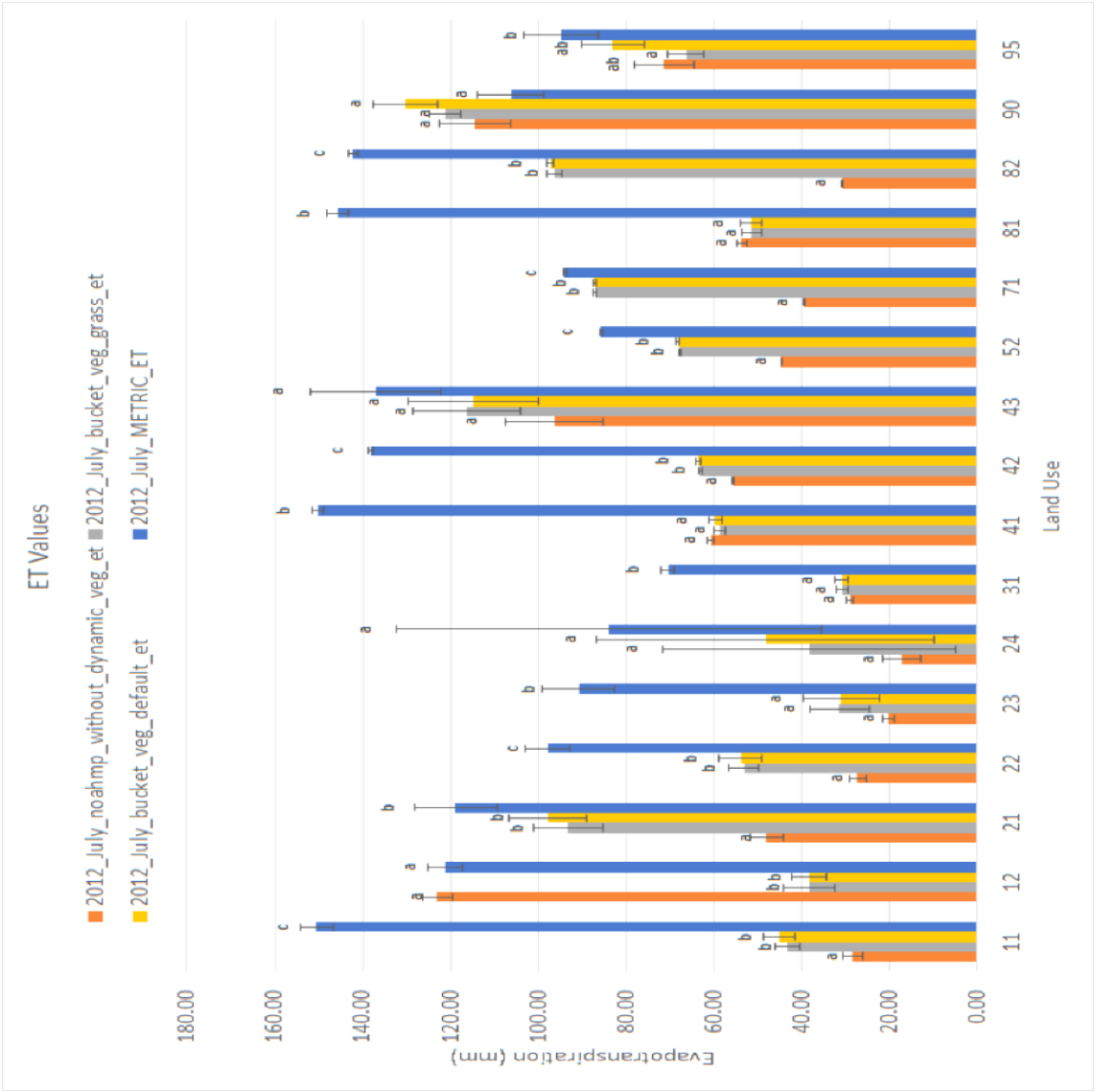

Figure 43. ET values for METRIC and different land surface models coupled with WRF for July, 2012

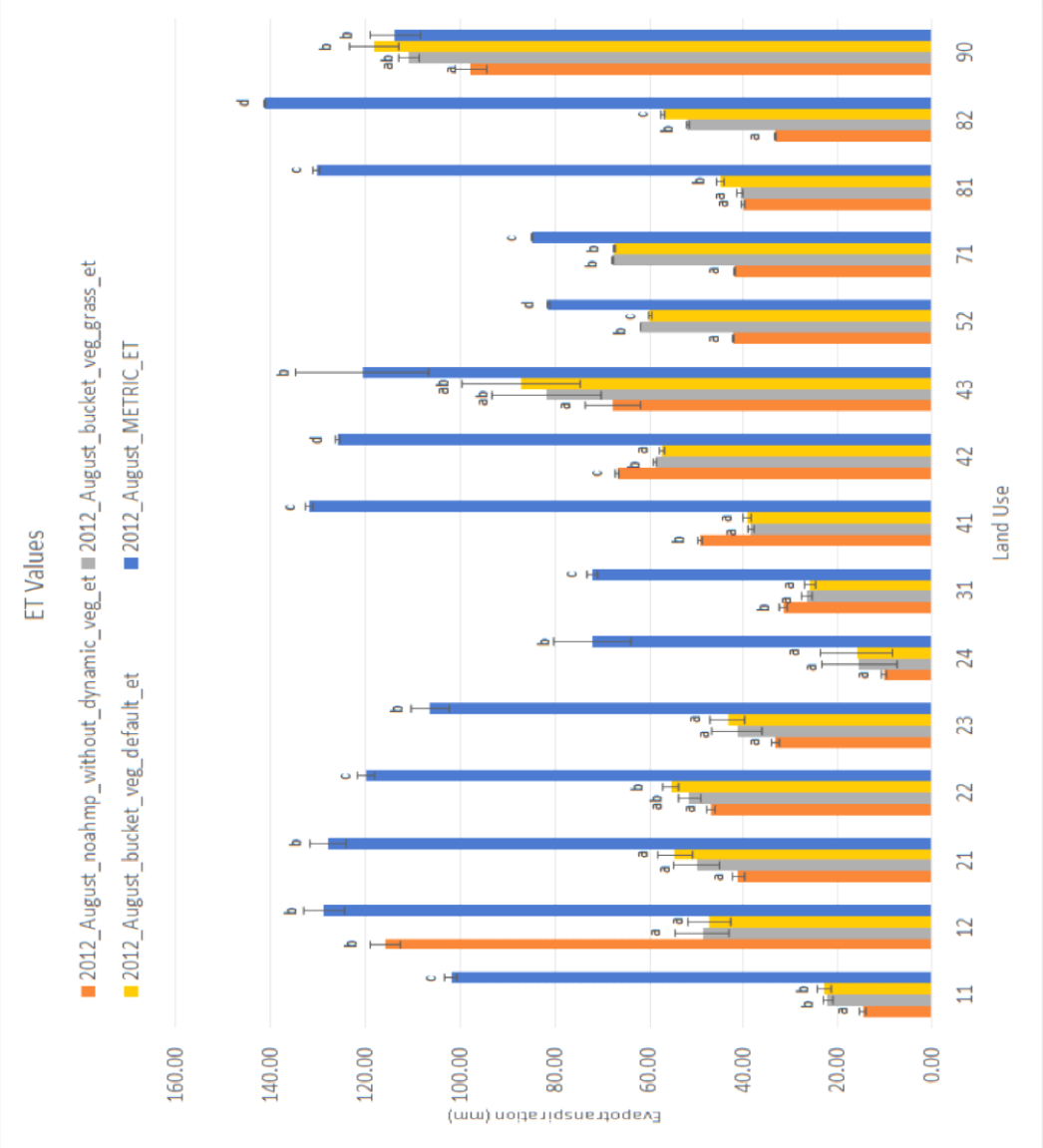

Figure 44. ET values for METRIC and different land surface models coupled with WRF for August, 2012

Global means and standard deviations are given for the models in Table 2 and Table 3. All the pixels which did not have a value for METRIC were eliminated and not included in the statistics. Based on these results it can be seen that overall METRIC estimates higher ET results. For 2012 which was a dry year, METRIC seems to overestimate ET. One should expect lower ET results for the dry year compared to the wet year. Bucket model is also insensitive to drought conditions. Noah-MP on the other hand generated lower values that shows it is more sensitive to drought conditions.

		2005	
	Models	Mean	Standard Dev
May	METRIC	110.54	30.19
	CLM	72.97	23.04
June	METRIC	128.53	46.69
	CLM	74.46	37.29
July	METRIC	130.23	46.91
	CLM	68.92	30.07
August	METRIC	96.45	33.97
	CLM	72.38	35.02

Table 2. Global mean values and standard deviations for CLM and METRIC

		2007		2012	
	Models	**Mean**	**Standard D**	**Mean**	**Standard D**
May	METRIC	121.77	32.90	115.77	44.28
	Noah-MP	93.62	33.70	56.12	34.15
	Bucket-Def	77.18	38.47	86.77	27.45
	Bucket-Gra	71.39	36.04	83.50	26.77
June	METRIC	129.69	52.93	116.06	52.94
	Noah-MP	95.56	33.13	47.19	22.64
	Bucket-Def	75.92	39.51	97	32.75
	Bucket-Gra	71.50	36.79	93.72	31.93
July	METRIC	116.38	46.87	100.17	42.24
	Noah-MP	92.78	35.47	54.49	31.40
	Bucket-Def	78.58	33.05	86.15	35.24
	Bucket-Gra	71.19	30.31	85.52	34.54
August	METRIC	102.51	36.85	102.84	41.91
	Noah-MP	70.59	33.72	53.03	31.30
	Bucket-Def	65.62	38.34	72.23	34.32
	Bucket-Gra	65.31	38.01	71.78	35.13

Table 3. Global mean values and standard deviations for different models

4.3. Validation of MODIS METRIC

Three Landsat derived ETrF images were selected to validate the MODIS ETrF images. The results showed MODIS simulations were reliable compared to Landsat imagery which has been validated with ground data. Figure 45 -50 shows the validation datasets. The validation runs are conducted for the Central Platte area for 2011 and 2013.

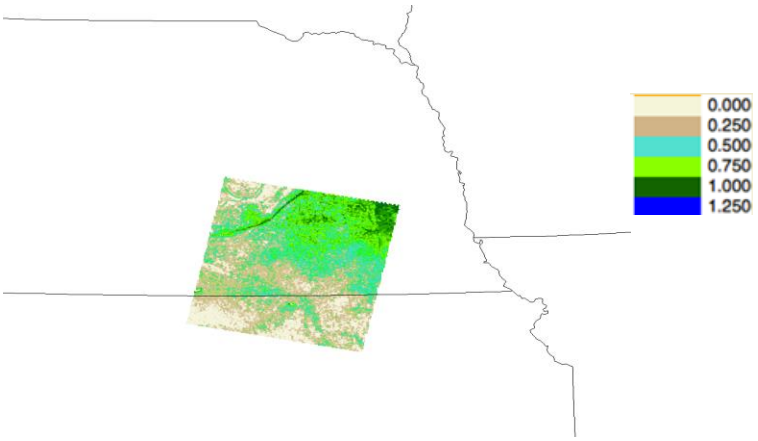

Figure 45. MODIS ETrF map (clipped with Landsat) for June 29, 2011.

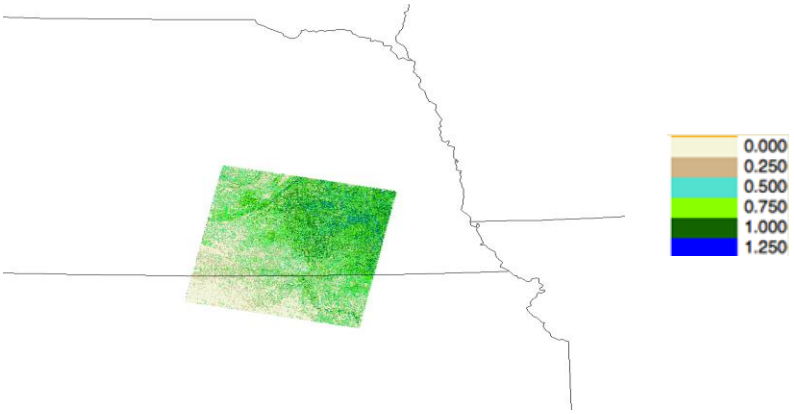

Figure 46. Landsat 7 ETrF map for June 29, 2011.

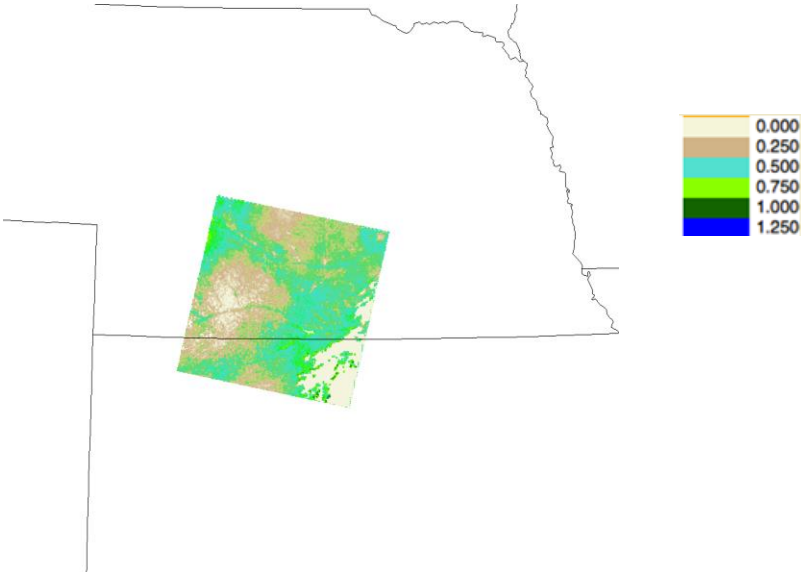

Figure 47. MODIS ETrF map (clipped with Landsat) for July 22, 2011.

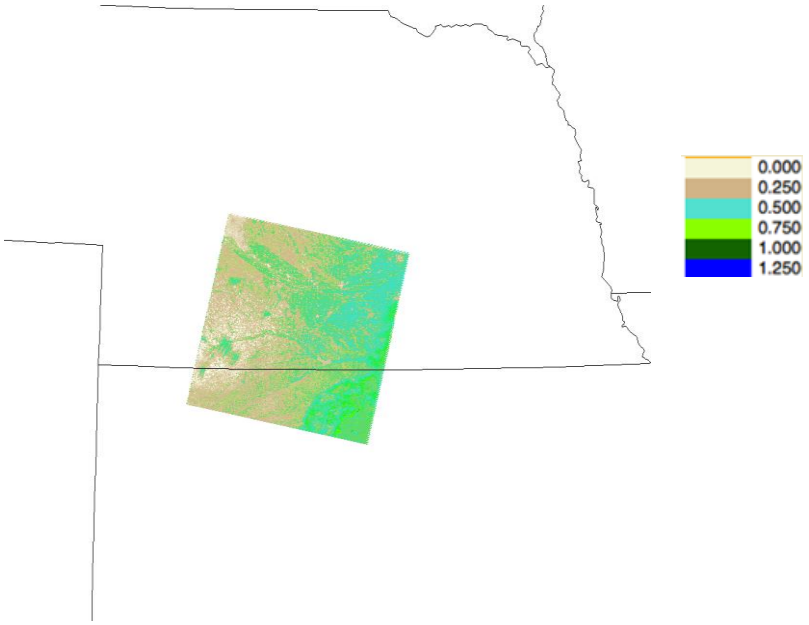

Figure 48. Landsat 7 ETrF map for July 22, 2011.

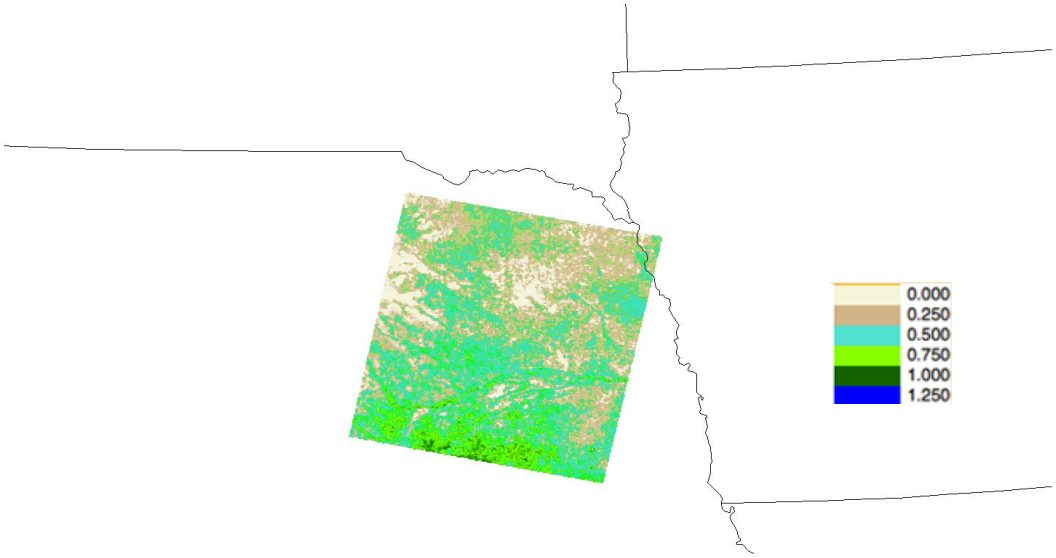

Figure 49. MODIS ETrF map (clipped with Landsat) for July 22, 2013.

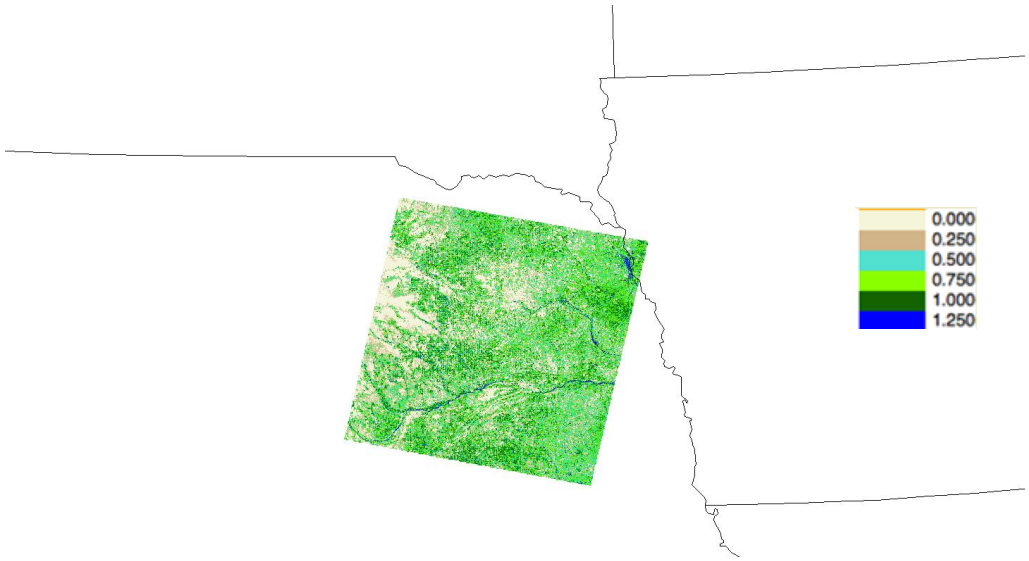

Figure 50. Landsat 7 ETrF map for July 22, 2013.

CHAPTER 5: CONCLUSION

This study evaluates different land surface models to determine, which model generates the closest result to the METRIC model. Based on the results it can be concluded that WRF coupled with CLM or Noah-MP generates the best results. However, for the dry year which is 2012, bucket model performed better than Noah-MP. There may be various reasons why models performs differently. One obvious reason of underestimation may be the irrigation. Irrigation is almost half of the input that enters into the hydrological system in some states, such as Nebraska. When irrigation is considered, the amount of soil moisture dramatically increases. The effects of irrigation can be seen all over the domain. Atmospheric circulation distributes the effect of irrigation to the surrounding regions according to Lu et al., 2015.

The increase in the soil moisture should reduce the surface temperature by evaporative cooling, which might be the reason for the warm-bias in WRF for Midwest. One other reason for the warm bias can be low LAI values generated by CLM and Noah-MP. Both models have a static LAI product which does not change year by year which may cause unrealistic results for extreme years such as 2012. In the surface physics models LAI controls the partitioning of transpiration from plants and evaporation from soils. According to Lu and Kueppers, 2012 WRF-CLM does not underestimate latent heat fluxes. If underestimation of latent heat flux is not the case for the low evapotranspiration values, there are two possibilities. One is low LAI values which generate greater evaporation compared to transpiration which yields low ET values. According to Lascano

et al., 1987, for agricultural fields 30 % of the ET is soil evaporation and the rest is transpiration. In order to have a reasonable ratio of evaporation and transpiration, LAI should be accurate since it controls the partitioning. Without sufficient soil moisture, neither accuracy of LAI, nor accuracy of latent heat flux matters since there is not enough moisture to evaporate in the soil. In order to effectively fix the ET problem, the priority should be adding the irrigation, and getting accurate LAI. One other effect of irrigation is, since the wet soil will be darker, albedo will decrease which will result higher net solar radiation.

Mixed pixels can be another cause of the low ET. Estimation of latent heat flux with multiple land use classes, roughness and soil moisture can yield deviations from the in-situ measurements. Kustas et al., 2004 found a trend of decreasing variance with coarser resolution and stated that the optimal pixel size should not be greater than 500 m for accurate latent heat flux estimations. One other difference between WRF and MODIS is the land surface temperature products (skin temperature for WRF). According to Sohrabinia et al., 2012 WRF skin temperature product has a better correlation with in-situ measurements compared to MODIS land surface temperature.

Further analyses are needed to pinpoint the exact reason of this behavior. All the major components of the surface energy balance should be checked in daily or even hourly time steps to see which product causes this problem.

REFERENCES

Allen, R. G., Pruitt, W. O., Raes, D., Smith, M., & Pereira, L. S. (2005). Estimating evaporation from bare soil and the crop coefficient for the initial period using common soils information. Journal of irrigation and drainage engineering, 131(1), 14-23.

Allen, R. G., Tasumi, M., & Trezza, R. (2007). Satellite-based energy balance for mapping evapotranspiration with internalized calibration (METRIC)—Model. Journal of irrigation and drainage engineering, 133(4), 380-394.

Allen, R. G., Tasumi, M., Morse, A., Trezza, R., Wright, J. L., Bastiaanssen, W., ... & Robison, C. W. (2007). Satellite-based energy balance for mapping evapotranspiration with internalized calibration (METRIC)—Applications. Journal of Irrigation and Drainage Engineering, 133(4), 395-406.

Bastiaanssen, W. G. M., Menenti, M., Feddes, R. A., & Holtslag, A. A. M. (1998). A remote sensing surface energy balance algorithm for land (SEBAL). 1. Formulation. Journal of hydrology, 212, 198-212.

Bethenod, O., Katerji, N., Goujet, R., Bertolini, J. M., & Rana, G. (2000). Determination and validation of corn crop transpirationby sap flow measurement under field conditions. Theoretical and Applied Climatology, 67(3-4), 153-160.

Bukovsky, M. S., & Karoly, D. J. (2007). A brief evaluation of precipitation from the North American Regional Reanalysis. Journal of Hydrometeorology, 8(4), 837-846.

Cai, X., Yang, Z. L., Xia, Y., Huang, M., Wei, H., Leung, L. R., & Ek, M. B. (2014). Assessment of simulated water balance from Noah, Noah-MP, CLM, and VIC over CONUS using the NLDAS test bed. Journal of Geophysical Research: Atmospheres, 119(24), 13-751.

Daly, C., R.P. Neilson, and D.L. Phillips. 1994. A statistical-topographic model for mapping climatological precipitation over mountainous terrain. J. Appl. Meteor., 33, 140-158.

Daly, C., Taylor, G. H., & Gibson, W. P. (1997, October). The PRISM approach to mapping precipitation and temperature. In Proc., 10th AMS Conf. on Applied Climatology (pp. 20-23).

DiLuzio, M., G.L. Johnson, C. Daly, J.K. Eischeid, and J.G. Arnold. 2008. Constructing retrospective gridded daily precipitation and temperature datasets for the conterminous United States. Journal of Applied Meteorology and Climatology, 47: 475-497

Dudhia, J. (1996, July). A multi-layer soil temperature model for MM5. In Preprint from the Sixth PSU/NCAR Mesoscale Model Users' Workshop (pp. 22-24).

Gao, B. C. (1996). NDWI—a normalized difference water index for remote sensing of vegetation liquid water from space. Remote sensing of environment, 58(3), 257-266.

Grant, N., L. Saito, M. Weltz, M. Walker, C. Daly, K. Stewart, and C. Morris. 2013. Instrumenting wildlife water developments to collect hydrometerological data in remote western U.S. catchments. Journal of Atmospheric and Oceanic Technology 30, 1161-1170.

Homer, C. H., Fry, J. A., & Barnes, C. A. (2012). The national land cover database. US Geological Survey Fact Sheet, 3020(4), 1-4.

Kustas, W. P., Li, F., Jackson, T. J., Prueger, J. H., MacPherson, J. I., & Wolde, M. (2004). Effects of remote sensing pixel resolution on modeled energy flux variability of croplands in Iowa. Remote sensing of Environment, 92(4), 535-547.

Lascano, R. J., Van Bavel, C. H. M., Hatfield, J. L., & Upchurch, D. R. (1987). Energy and water balance of a sparse crop: simulated and measured soil and crop evaporation. Soil Science Society of America Journal, 51(5), 1113-1121.

Lu, Y., & Kueppers, L. M. (2012). Surface energy partitioning over four dominant vegetation types across the United States in a coupled regional climate model (Weather Research and Forecasting Model 3–Community Land Model 3.5). Journal of Geophysical Research: Atmospheres (1984–2012), 117(D6).

Lu, Y., Jin, J., & Kueppers, L. M. (2015). Crop growth and irrigation interact to influence surface fluxes in a regional climate-cropland model (WRF3. 3-CLM4crop). Climate Dynamics, 1-17.

McCoy, R., Jin, J., & Wang, S. Y. S. (2010). Evaluation of a coupled WRF-CLM model over the western United States.

Mesinger, F., DiMego, G., Kalnay, E., Mitchell, K., Shafran, P. C., Ebisuzaki, W., ... & Shi, W. (2006). North American regional reanalysis. Bulletin of the American Meteorological Society, 87(3), 343-360.

Michalakes, J., Dudhia, J., Gill, D., Henderson, T., Klemp, J., Skamarock, W., & Wang, W. (2004, October). The weather research and forecast model: software architecture and performance. In Proceedings of the 11th ECMWF Workshop on the Use of High Performance Computing In Meteorology (Vol. 25, p. 29). Reading, UK.

Mitchell, K. E., Lohmann, D., Houser, P. R., Wood, E. F., Schaake, J. C., Robock, A., ... & Bailey, A. A. (2004). The multi-institution North American Land Data Assimilation System (NLDAS): Utilizing multiple GCIP products and partners in a continental distributed hydrological modeling system. Journal of Geophysical Research: Atmospheres (1984–2012), 109(D7).

Mu, Q., Heinsch, F. A., Zhao, M., & Running, S. W. (2007). Development of a global evapotranspiration algorithm based on MODIS and global meteorology data. Remote Sensing of Environment, 111(4), 519-536.

Myneni, R. B., Asrar, G., Tanre, D. I. D. I. E. R., & Choudhury, B. J. (1992). Remote sensing of solar radiation absorbed and reflected by vegetated land surfaces. Geoscience and Remote Sensing, IEEE Transactions on, 30(2), 302-314.

Niu, G. Y., Yang, Z. L., Mitchell, K. E., Chen, F., Ek, M. B., Barlage, M., ... & Xia, Y. (2011). The community Noah land surface model with multiparameterization options (Noah-MP): 1. Model description and evaluation with local-scale measurements. Journal of Geophysical Research: Atmospheres (1984–2012), 116(D12).

Oleson, K. W., Lawrence, D. M., Gordon, B., Flanner, M. G., Kluzek, E., Peter, J., ... & Zeng, X. (2010). Technical description of version 4.0 of the Community Land Model (CLM).

Schwarz, G. E., & Alexander, R. B. (1995). State Soil Geographic (STATSGO) data base for the conterminous United States (No. 95-449).

Sohrabinia, M., Rack, W., & Zawar-Reza, P. (2012). Analysis of MODIS LST compared with WRF model and in situ data over the Waimakariri River basin, Canterbury, New Zealand. Remote Sensing, 4(11), 3501-3527.

Trezza, R., Allen, R. G., & Tasumi, M. (2013). Estimation of actual evapotranspiration along the Middle Rio Grande of New Mexico using MODIS and Landsat imagery with the METRIC Model. Remote Sensing, 5(10), 5397-5423.

Tucker, C. J. (1979). Red and photographic infrared linear combinations for monitoring vegetation. Remote sensing of Environment, 8(2), 127-150.

Walter, I. A., Allen, R. G., Elliott, R., Jensen, M. E., Itenfisu, D., Mecham, B., ... & Martin, D. (2000, November). ASCE's standardized reference evapotranspiration equation. In Proc. of the Watershed Management 2000 Conference, June.

Wickham, J. D., Stehman, S. V., Gass, L., Dewitz, J., Fry, J. A., & Wade, T. G. (2013). Accuracy assessment of NLCD 2006 land cover and impervious surface. Remote Sensing of Environment, 130, 294-304.